THE GEOLOGICAL SOCIETY OF AMERICA®

The stability of dinosaur communities before the Cretaceous–Paleogene (K–Pg) boundary: A perspective from southern Alberta using calcium isotopes as a dietary proxy

Jeremy E. Martin[1,†], Auguste Hassler[1], Gilles Montagnac[1], François Therrien[2], and Vincent Balter[1]
[1]*Centre National de la Recherche Scientifique UMR 5276, LGLTPE, Université de Lyon, ENS de Lyon, Université Lyon 1, 46 Allée d'Italie, 69342 Lyon Cedex 07, France*
[2]*Royal Tyrrell Museum of Palaeontology, Drumheller, Alberta T0J 0Y0, Canada*

ABSTRACT

Reconstructing dinosaur trophic structure prior to the Cretaceous–Paleogene (K–Pg) boundary may provide information about ecosystem organization and evolution. Using calcium isotopes, we investigate preserved biogenic isotope compositions in a set of dinosaur teeth from three continental formations from Alberta, Canada, to assess latest Cretaceous food web structure. Tooth enamel $\delta^{44/42}$Ca values are presented for tyrannosaurids (n = 34) and potential large herbivorous prey (n = 42) in the upper Campanian Dinosaur Provincial Park Formation, uppermost Campanian–Maastrichtian Horseshoe Canyon Formation, and upper Maastrichtian–lower Paleocene Scollard Formation, spanning the last ~10 m.y. of the Cretaceous. The influence of diagenesis is assessed in a subset sample through major and trace elemental concentrations and ultraviolet (UV) Raman spectra, which provides a framework for interpreting calcium isotope values. In the Dinosaur Park Formation, hadrosaurid $\delta^{44/42}$Ca values are systematically heavier than ceratopsid values, a difference that is interpreted to reflect niche partitioning among megaherbivores. Tyrannosaurid $\delta^{44/42}$Ca values are scattered but on average, they are ^{44}Ca-depleted relative to herbivorous dinosaurs in all three formations. As interpreted from the Dinosaur Park data set, tyrannosaurids may have preferentially fed on hadrosaurids. These analyses offer possibilities for testing whether trophic structure among non-avian dinosaur ecosystems changed several millions of years prior to the K–Pg boundary.

INTRODUCTION

The latest Cretaceous fossil record of North America offers one of the best preserved, quasi-continuous records of dinosaur-dominated ecosystems spanning the Campanian–Maastrichtian interval and is thus ideal for paleoecological studies at different timescales. Apex predators, represented by tyrannosaurids, dominated terrestrial ecosystems. Numerous potential megaherbivore prey species—namely hadrosaurids and ceratopsids—lived continuously during this time interval (Mallon et al., 2012; Eberth et al., 2013). But whether dinosaur faunal successions were accompanied by significant modifications of the consumer-prey relationship is unknown, and this hinders our understanding of ecological perturbation in dinosaur communities prior to the Cretaceous–Paleogene (K–Pg) boundary.

How the terrestrial ecosystem functioned during the Late Cretaceous in North America has been explored from the perspective of niche partitioning and ecological specialization using different approaches that include dinosaur biostratigraphy and ecomorphospace analysis (Mallon et al., 2012), biometrics (Mallon et al., 2013; Mallon and Anderson, 2013), dental morphology and microwear (Erickson et al., 2012; Mallon and Anderson, 2014; Erickson et al., 2015), light stable isotopes (Ostrom et al., 1993; Fricke and Pearson, 2008; Fricke et al., 2008, 2009; Frederickson et al., 2018; Cullen et al., 2020), and radiogenic strontium isotopes (Terrill et al., 2020). Using a food web model, Mitchell et al. (2012) observed a shift in trophic structure between Campanian and Maastrichtian communities in North America and recovered highly connected guilds for the latest stage, thus implying that the ecosystem was more sensitive to environmental perturbations. Models, such as those employed by Mitchell et al. (2012), are dependent upon links among different members of fossil communities. Assumptions used in the making of these models rely on the various types of studies mentioned above.

In the case of isotopic analyses, paleoecological inferences are established based on the isotopic proxy implemented as measured from fossil bioapatite. Among the widely used proxies, oxygen isotopes provide information on body water cycle and allow for derivation of the δ^{18}O value of the drinking water and the temperature at which bioapatite minerals precipitated, which permits a reconstruction of habitat use and physiology (e.g., Kohn et al., 1996). Information about carbon cycling in the environment retrieved from carbon isotopes allows inferences to be made about plant resource use by herbivores (DeNiro and Epstein, 1978). However, dietary specializations become challenging to detect in C3-dominated ecosystems, while open versus closed habitats or canopy-related fractionation can be determined (van der Merwe and Medina, 1989; Cerling et al., 2004). The carbonate fraction of enamel bioapatite has good preservation potential, and several studies have investigated niche partitioning among herbivorous dinosaurs by using carbon isotopes (e.g., Fricke and Pearson, 2008; Tütken, 2011; Amiot et al., 2015; Cullen et al., 2020).

The isotopic toolkit available for paleoecological research is expanding with continual improvement in analytical methods. New methods now permit the measurement of non-traditional isotopes in fossil bioapatite such as calcium, magnesium, and zinc (e.g., Martin et al., 2015; Jaouen et al., 2016; Martin et al., 2017a, 2017b; Hassler et al., 2018; Bourgon et al., 2020; Tacail et al., 2020), or light isotopes, such as nitrogen (Ostrom et al., 1993), that can be preserved in tooth enamel (Leichliter et al., 2020). With regards to transition metals, the choice of the isotopic proxy to be used remains dictated by its concentration in fossil bioapatite. In other words, to the detriment of fossil integrity, the smaller the concentration of

Jeremy E. Martin http://orcid.org/0000-0001-9159-645X
[†]jeremy.martin@cnrs.fr.

GSA Bulletin;
published online 10 February 2022
https://doi.org/10.1130/B36222.1; 4 figures; 2 tables.

a given element, the larger the amount of sample required. In addition, trace metals may be prone to adsorption or substitution processes during diagenesis and, when possible, quality-control concentration analyses should be implemented prior to measuring their isotopic content (e.g., Kohn et al., 1999; Trueman and Tuross, 2002; Kohn et al., 2013; Reynard and Balter, 2014).

Calcium is an essential element for vertebrate metabolism, and although its regulation in the body is not fully understood (see review in Tacail et al., 2020), there exists a constant offset from dietary calcium to bone, which supports the idea of a trophic level effect (Skulan and DePaolo, 1999; Chu et al., 2006, and references below). Calcium isotopes are therefore primarily used as a trophic proxy, as in studies of modern aquatic and terrestrial vertebrate food webs (e.g., Skulan et al., 1997; Clementz et al., 2003; Martin et al., 2015, 2018). Calcium in bioapatite presents the advantage of being highly concentrated, with more than 30 wt%, making it one of the most diagenetically resistant elements in that tissue, and it is nearly immune to pore-fluid remobilization as modeled using a simple mass-balance (Martin et al., 2017a). However, calcium and other metals can be altered in dentine and to some extent in enamel, as evidenced from controlled in vitro alteration experiments in acidic aqueous solutions (Weber et al., 2021); hence, bioapatite alteration needs to be assessed in fossil bioapatite. Where trace elements require several milligrams of bioapatite, measurements of calcium isotopes require ~200 μg of material, which allows for minimal destruction and allows for a broader sampling of specimens.

Here, we build on previous investigations of the calcium isotopic composition of dinosaur bioapatite (Heuser et al., 2011; Hassler et al., 2018), assess its biogenic integrity using concentration analyses and Raman spectroscopy, and present a large calcium isotopic data set for dinosaur assemblages of Alberta, Canada, spanning the last 10 m.y. of the Cretaceous (Fig. 1). A focus on tyrannosaurids and their potential herbivorous prey allows investigation of whether changes in trophic organization occurred among these dinosaur communities prior to the K–Pg boundary.

The present study aims primarily to (1) detect any taxonomic differences at a broad resolution (i.e., formation-level) and (2) provide upper and lower bounds to the isotopic variability recorded in each dinosaur family. Although fine-scale dietary preferences cannot be detected with the data set at hand, such results show encouraging perspectives for applying calcium isotope research among Mesozoic vertebrate communities at the scale of the individual and when available, at the scale of a single stratigraphic unit (e.g., faunal assemblage zone, constrained stratigraphic horizon, multi-taxic bonebed). The aim of this study was also to be as minimally destructive as possible. Using such very small (sub-milligram) amounts, most of the teeth sampled did not yield enough enamel to surpass the detection limits of trace elements, which include rare earth elements (REE). Therefore, the diagenetic results obtained for a subset of samples do not reflect a systematic understanding of the whole data set. This should be kept in mind when discussing outliers, because the absence of diagenesis is not proven for all individual samples per se.

GEOLOGY AND AGE

Dinosaur teeth were selected from three Upper Cretaceous continental rock formations in the Western Canada Basin, which is a foreland basin that formed in response to the uplift of the Rocky Mountains in western North America (Cant and Stockmal, 1989; Catuneanu et al., 2000). These three rock formations, the Dinosaur Park Formation, the Horseshoe Canyon Formation, and the Scollard Formation, were deposited between the Upper Campanian and lower Paleocene as part of a series of eastward-thinning, clastic wedges separated by marine deposits of the Bearpaw Formation (Eberth, 2005; Eberth and Braman, 2012; Eberth and Kamo, 2019, 2020). Together, they preserve a rich fossil record for the last ~10 m.y. of the Cretaceous.

Dinosaur Park Formation

Specimens analyzed in this study (Table 1) were collected between 1964 and 2011 from exposures of the ~75-m-thick upper Campanian Dinosaur Park Formation in Dinosaur Provincial Park (DPP), a UNESCO World Heritage site located along a stretch of the Red Deer River

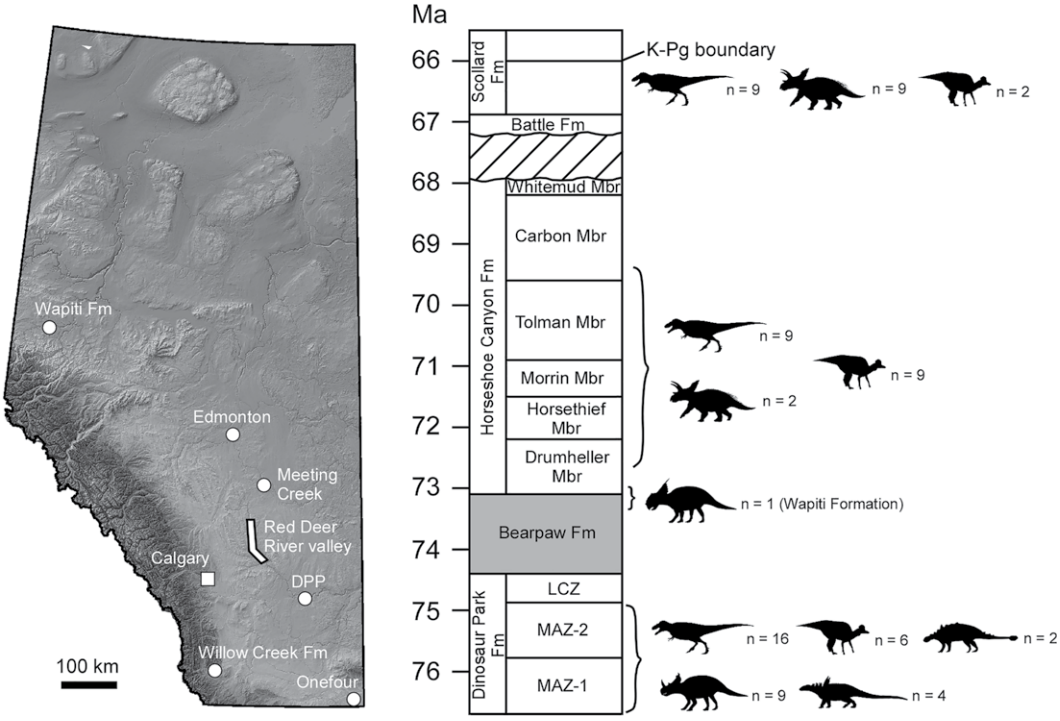

Figure 1. Geographic distribution of various fossil localities within the province of Alberta, Canada, and the stratigraphic distribution of dinosaur specimens studied are shown. See Table 1 for a compilation of provenance data for all specimens analyzed in this study. LCZ—Lethbridge Coal Zone; MAZ—megaherbivore assemblage zone; DPP—Dinosaur Provincial Park; Fm—formation; Mbr—member. Dinosaur silhouettes are from Phylopic.org.

TABLE 1. DINOSAUR TEETH AND STANDARDS CALCIUM ISOTOPE VALUES ANALYZED IN THIS STUDY

Specimen number	Taxon	Stratigraphic position	Number of measurements	$\delta^{44/42}$Ca (‰) rel. ICP Ca Lyon	$\delta^{43/42}$Ca (‰) rel. ICP Ca Lyon	$\delta^{44/42}$Ca_2SD (‰) rel. ICP Ca Lyon	$\delta^{43/42}$Ca_2SD (‰) rel. ICP Ca Lyon	$\delta^{44/42}$Ca (‰) rel. SRM_915a
Scollard Formation (66.88–66 Ma)								
TMP1991.170.7	Ceratopsidae	upper	4	–0.84	–0.46	0.20	0.21	–0.33
TMP1993.88.2	Ceratopsidae	upper	5	–0.94	–0.46	0.07	0.02	–0.42
TMP2002.71.25	Ceratopsidae	~3 m below K–Pg boundary	4	–0.89	–0.47	0.06	0.08	–0.37
TMP2009.13.105	Ceratopsidae	upper	4	–0.86	–0.44	0.04	0.03	–0.34
TMP2009.152.5	Ceratopsidae	middle	5	–0.94	–0.47	0.17	0.15	–0.42
TMP2011.8.3	Ceratopsidae	lower	4	–0.94	–0.52	0.08	0.10	–0.43
TMP2015.40.184	Ceratopsidae	middle?	5	–0.97	–0.49	0.13	0.09	–0.45
TMP2015.8.22	Ceratopsidae	upper	4	–1.01	–0.55	0.09	0.06	–0.49
TMP2014.8.21	Hadrosauridae	upper	4	–0.77	–0.42	0.09	0.06	–0.25
TMP2014.8.7	Hadrosauridae	upper	4	–0.77	–0.45	0.08	0.08	–0.25
TMP1994.31.5	Tyrannosauridae	lower	5	–1.18	–0.60	0.06	0.03	–0.67
TMP1998.5.3	Tyrannosauridae	base	4	–1.41	–0.74	0.12	0.07	–0.89
TMP1998.8.24	Tyrannosauridae	base	4	–0.96	–0.55	0.09	0.07	–0.44
TMP1998.8.56	Tyrannosauridae	upper?	4	–0.80	–0.44	0.11	0.07	–0.29
TMP2014.8.19	Tyrannosauridae	upper	5	–0.99	–0.54	0.17	0.16	–0.47
TMP2014.8.20	Tyrannosauridae	upper	5	–0.66	–0.32	0.12	0.12	–0.14
TMP2014.8.6	Tyrannosauridae	upper	3	–1.11	–0.56	0.06	0.04	–0.59
TMP2015.8.16	Tyrannosauridae	upper	5	–0.95	–0.48	0.07	0.08	–0.43
TMP1981.6.1 (Willow Creek Fm)	Tyrannosauridae	Scolllard equivalent	4	–1.25	–0.64	0.09	0.10	–0.73
Horseshoe Canyon Formation (73.1–67.95 Ma)								
TMP1990.82.42 (in Edmonton)	Ceratopsidae	Horsethief Member	2	–0.87	–0.47	0.05	0.01	–0.36
TMP2003.61.4	Ceratopsidae	Tolman Member	2	–0.52	–0.27	0.07	0.12	0.00
TMP2003.62.3	Ceratopsidae	Tolman Member	4	–0.65	–0.35	0.05	0.09	–0.13
TMP1965.16.152	Hadrosauridae	Horsethief-Morrin Members	2	–0.82	–0.44	0.03	0.06	–0.30
TMP1965.16.154	Hadrosauridae	Horsethief-Morrin Members	1	–0.60	–0.33	–	–	–0.09
TMP1965.16.156	Hadrosauridae	Horsethief-Morrin Members	3	–0.10	–0.03	0.09	0.08	0.42
TMP1965.16.158	Hadrosauridae	Drumheller Member	2	–0.35	–0.18	0.05	0.03	0.17
TMP1965.16.160	Hadrosauridae	Drumheller Member	2	–0.75	–0.41	0.00	0.02	–0.23
TMP1965.16.161	Hadrosauridae	Drumheller Member	2	–0.69	–0.35	0.05	0.01	–0.17
TMP1985.12.24	Hadrosauridae	Horsethief Member	3	–0.84	–0.46	0.00	0.11	–0.32
TMP1990.2.34	Hadrosauridae	Tolman-Carbon Member	3	–0.94	–0.54	0.03	0.06	–0.42
TMP1997.77.1	Hadrosauridae	Drumheller Member	1	–0.43	–0.18	–	–	0.09
TMP1981.31.68	Tyrannosauridae	Morrin-Tolman Members	1	–0.92	–0.49	–	–	–0.40
TMP1984.163.23 (in Edmonton)	Tyrannosauridae	Horsethief-Morrin Members	2	–1.02	–0.52	0.05	0.03	–0.51
TMP1986.209.07	Tyrannosauridae	Drumheller Member	2	–1.48	–0.81	0.01	0.07	–0.96
TMP1986.209.10	Tyrannosauridae	Drumheller Member	1	–1.04	–0.55	–	–	–0.52
TMP1989.17.33 (in Edmonton)	Tyrannosauridae	Horsethief Member	3	–1.20	–0.62	0.06	0.11	–0.68
TMP1991.63.18 (in Edmonton)	Tyrannosauridae	Horsethief Member	2	–1.20	–0.60	0.05	0.06	–0.68
TMP1994.7.1 (at Meeting Creek)	Tyrannosauridae	lower?	3	–0.96	–0.47	0.04	0.02	–0.45
TMP1998.64.3	Tyrannosauridae	Tolman Member	4	–1.10	–0.56	0.10	0.13	–0.59
TMP1989.55.218 (Wapiti Fm)	Tyrannosauridae	Upper Bearpaw-lower HSC equivalent	4	–1.10	–0.56	0.08	0.06	–0.58
Dinosaur Park Formation (ca. 76.5–74.4 Ma)								
TMP1981.14.12	Ankylosauridae	?	2	–0.78	–0.42	0.08	0.05	–0.26
TMP1998.68.153	Ankylosauridae	Low	2	–0.90	–0.46	0.02	0.05	–0.38
TMP1987.36.250	Ceratopsidae	middle?	4	–1.00	–0.52	0.14	0.08	–0.48
TMP1987.36.65	Ceratopsidae	?	4	–0.81	–0.42	0.07	0.06	–0.29
TMP1993.150.18	Ceratopsidae	Lower	4	–1.06	–0.53	0.06	0.07	–0.54
TMP1994.12.238	Ceratopsidae	?	4	–0.97	–0.49	0.08	0.06	–0.45
TMP1994.12.44	Ceratopsidae	Low	2	–1.01	–0.51	0.07	0.04	–0.49
TMP1994.376.19	Ceratopsidae	middle?	2	–1.32	–0.66	0.04	0.04	–0.81
TMP1999.55.66	Ceratopsidae	middle?	2	–1.27	–0.63	0.16	0.09	–0.75
TMP2000.12.38	Ceratopsidae	Upper	3	–1.14	–0.57	0.06	0.04	–0.62
TMP2000.12.39	Ceratopsidae	lower?	4	–0.90	–0.47	0.08	0.04	–0.38
TMP1979.14.563	Hadrosauridae	middle?	2	–0.71	–0.38	0.13	0.07	–0.19
TMP1980.16.1066	Hadrosauridae	Low	2	–0.82	–0.41	0.09	0.09	–0.30
TMP1980.20.174	Hadrosauridae	Lower	3	–0.69	–0.36	0.06	0.05	–0.17
TMP1980.44.12	Hadrosauridae	?	4	–0.67	–0.34	0.15	0.08	–0.15
TMP1980.44.12	Hadrosauridae	?	4	–0.59	–0.32	0.12	0.06	–0.07
TMP1980.8.161	Hadrosauridae	?	4	–0.60	–0.31	0.10	0.08	–0.08
TMP1968.4.6	Nodosauridae	?	3	–0.94	–0.53	0.05	0.03	–0.42
TMP1994.12.39	Nodosauridae	low?	3	–1.05	–0.54	0.03	0.05	–0.53
TMP2011.47.2 (at Onefour)	Nodosauridae	<10 m below Lethbridge Coal Zone	2	–0.98	–0.50	0.15	0.05	–0.46
TMP1981.27.19	Tyrannosauridae	middle?	2	–0.98	–0.49	0.17	0.08	–0.46
TMP1982.19.330	Tyrannosauridae	?	3	–1.24	–0.62	0.07	0.06	–0.72
TMP1986.18.42	Tyrannosauridae	Lower	2	–1.07	–0.54	0.17	0.07	–0.55
TMP1992.36.1065	Tyrannosauridae	Low	4	–1.08	–0.55	0.18	0.12	–0.56
TMP1992.36.238	Tyrannosauridae	middle?	3	–1.09	–0.56	0.10	0.08	–0.57

(*Continued*)

TABLE 1. *CONTINUED*

Specimen number	Taxon	Stratigraphic position	Number of measurements	$\delta^{44/42}$Ca (‰) rel. ICP Ca Lyon	$\delta^{43/42}$Ca (‰) rel. ICP Ca Lyon	$\delta^{44/42}$Ca_2SD (‰) rel. ICP Ca Lyon	$\delta^{43/42}$Ca_2SD (‰) rel. ICP Ca Lyon	$\delta^{44/42}$Ca (‰) rel. SRM_915a
TMP1992.36.976	Tyrannosauridae	?	4	−1.01	−0.53	0.13	0.11	−0.49
TMP1994.12.1007	Tyrannosauridae	?	2	−1.21	−0.60	0.15	0.07	−0.69
TMP2000.12.13	Tyrannosauridae	Upper	3	−1.14	−0.58	0.16	0.08	−0.62
TMP2000.12.63	Tyrannosauridae	Low	4	−1.15	−0.59	0.07	0.06	−0.64
TMP2000.12.7	Tyrannosauridae	middle?	2	−1.18	−0.60	0.06	0.00	−0.66
TMP2000.12.80	Tyrannosauridae	low?	2	−1.55	−0.76	0.21	0.12	−1.03
TMP2000.12.87	Tyrannosauridae	middle?	2	−1.14	−0.55	0.01	0.01	−0.62
TMP2003.12.276	Tyrannosauridae	Lower	2	−1.19	−0.57	0.13	0.03	−0.67
TMP2003.12.60	Tyrannosauridae	Low	4	−0.84	−0.42	0.15	0.09	−0.32
TMP2006.12.23	Tyrannosauridae	Middle	4	−1.17	−0.61	0.11	0.07	−0.65
TMP2011.12.39	Tyrannosauridae	Low	3	−1.01	−0.51	0.15	0.03	−0.49
Standards								
IAPSO dino1			2	0.42	0.24	0.05	0.02	0.94
IAPSO dino2			4	0.41	0.21	0.04	0.06	0.93
SRM1486 dino1			9	−1.03	−0.53	0.06	0.07	−0.52
SRM1486-(JM40-JM59)			11	−0.99	−0.51	0.15	0.07	−0.47
SRM1486-(JM60-JM80)			17	−1.00	−0.51	0.07	0.07	−0.49
SRM1486-19122018			17	−0.96	−0.49	0.11	0.11	−0.44

Note: ICP—inductively coupled plasma; SRM—standard reference material; Fm—formation; HSC—Horseshoe Canyon Formation.

in southern Alberta, where strata are exposed over a surface area of 75 km^2 (Eberth, 2005). One nodosaurid tooth comes from exposures of the same formation near the Onefour township agriculture research station in southeastern Alberta, approximately 200 km away (Fig. 1). The Dinosaur Park Formation represents a time interval between 76.5 Ma and 74.8 Ma (Eberth, 2005). Based on the average sedimentation rate of 4.1 cm/ka calculated by Eberth (2005), Mallon et al. (2012) estimated the duration of the two dinosaur biozones recognized in the formation (MAZ-1 and MAZ-2) at ~600 k.y. each. In terms of large dinosaurs (>1 t), at least two tyrannosaurid species, eight hadrosaurid species, six ceratopsid species, and three ankylosaur species are known from the Dinosaur Park Formation (Mallon et al., 2012). Because assignment of isolated teeth to a precise species of dinosaur is not possible, the question of niche partitioning at the specific level will therefore not be treated in the present study. GPS coordinates and locality information indicate that specimens were collected at various stratigraphic levels throughout the park, although precise stratigraphic position could not be determined in most cases (Fig. 1 and Table 1). Therefore, the Dinosaur Park dinosaur tooth sample is representative of a time window of ~1.2 m.y. (i.e., corresponding to the two biozones), whereas the entirety of the Dinosaur Park Formation is closer to a duration of 1.7 m.y.

Horseshoe Canyon Formation

Specimens were collected between 1965 and 2013 from exposures of the uppermost Campanian–Maastrichtian Horseshoe Canyon Formation along the Red Deer River valley in the general vicinity of Drumheller, near Meeting Creek, and in Edmonton in southcentral and central Alberta (Table 1, Fig. 1). The Horseshoe Canyon Formation is subdivided into four members that span a time interval of about 5 m.y. between 73.1 Ma and 68 Ma (Eberth and Kamo, 2020) and represents the longest time range in the sampling approach. One ceratopsid tooth, belonging to *Pachyrhinosaurus lakustai*, comes from a stratigraphic interval of the Wapiti Formation in northwestern Alberta, approximately 400 km from Edmonton, that is roughly time-equivalent to the contact between the Horseshoe Canyon Formation and the underlying marine Bearpaw Formation (Fig. 1; Eberth in Currie et al., 2008).

Scollard Formation

Specimens analyzed in this study come from different localities of the Cretaceous portion of the upper Maastrichtian–lower Paleocene Scollard Formation exposed northwest of Drumheller, Alberta, and were collected between 1964 and 2015 (Table 1, Fig. 1). The Cretaceous portion of the Scollard Formation spans between 66.88 Ma and 66.043 Ma, i.e., ~800 k.y. (Eberth and Kamo, 2019). One tyrannosaurid tooth comes from a time-equivalent interval of the Willow Creek Formation in southwestern Alberta approximately 300 km away (Fig. 1).

MATERIAL AND METHODS

Dinosaur Tooth Samples

Enamel from 75 individual tooth specimens was sampled using a microdrill device or, in some cases, using a stainless steel scalpel blade to detach enamel fragments (Table 1). For most teeth, enamel was sampled in the lower half of the crown. Tooth formation takes between 1 yr and 2.5 yr for tyrannosaurids and about 1 yr for ceratopsids and hadrosaurids (Erickson, 1996; D'Emic et al., 2019). Because enamel microdrill sampling spots are ~300 μm in diameter (i.e., roughly equivalent to 20 von Ebner increments in the adjacent dentine), the calcium isotope value measured for a single individual records a limited dietary event (i.e., days or weeks) and not an average diet over the whole tooth crown. However, the process of enamel maturation may contribute to a further time averaging as observed in the enamel of mammals (Passey and Cerling, 2002; Trayler and Kohn, 2017). Most specimens were collected at the ground surface and all were identified at the taxonomic family level. The data set includes teeth from tyrannosaurids (n = 16), hadrosaurids (n = 6), ceratopsids (n = 9), nodosaurids (n = 3), and ankylosaurids (n = 2) from the Dinosaur Park Formation; teeth from tyrannosaurids (n = 9), hadrosaurids (n = 9), and ceratopsids (n = 3) from the Horseshoe Canyon Formation (and time-equivalent Wapiti Formation of northwestern Alberta); and teeth from tyrannosaurids (n = 9), hadrosaurids (n = 2), and ceratopsids (n = 8) from the Scollard Formation (and time-equivalent Willow Creek Formation of southwestern Alberta) (Table 1, Fig. 1).

Raman Spectroscopy

The presence/absence of diagenetic secondary carbonates was assessed using Raman spectroscopy on three hadrosaurid tooth enamel samples from the Dinosaur Park, Horseshoe Canyon, and Scollard Formations, as well as on tooth enamel of a modern *Crocodylus niloticus* for comparison. Deep UV Resonant Raman (DUV-RR) spectroscopy was performed with a Horiba LabRAM HR800 UV system. The Raman diffusion was excited with 244 nm wavelength. A spe-

cially designed Mitutoyo™ SLWD 50× objective lens was used with a working distance of 11 mm to focus the laser on the samples, giving a probe spot of 3 μm diameter (Montagnac et al., 2016, 2021). This methodological approach permits clear resolution in the spectrum of bioapatite, where other Raman approaches used on fossil material often yield high luminescence of the background. The Raman spectra were recorded in the 400–1600 cm^{-1} wavelength range with a 3600 grooves/mm grating. This spectral range covers the Raman fingerprint of vibrations of phosphates and carbonates. Each spectrum is the average of 200 spectra collected during the scanning of a 100 × 100 μm^2 surface area. The full acquisition time is around 200 s. In the deep UV domain, no background was observed in the Raman spectra and no preprocessing was applied. The spectral peak positions were adjusted with the reference of the N_2 (2331 cm^{-1}) and O_2 Raman peaks (1555 cm^{-1}) detected during UV beam path in air. The Raman peaks associated with $\nu 1\text{-}PO_4^{3-}$ and B-type CO_3^{2-} were fitted with Voight spectral models with the Matlab application tool PeakFit (O'Haver, 2021).

Concentration Analyses, Purification and Isotopic Measurements

All samples were placed in Teflon beakers and fully digested using ultrapure, concentrated nitric acid (15 N) at 130 °C for 1 hr. Samples were then evaporated and re-dissolved in a solution of ultrapure nitric acid (0.5 N). The sample weights could not be assessed in most cases because of the risk of losing such small amounts of powder during transfers between vials and scale. Samples were purified following previously published protocols (Tacail et al., 2014). A number of samples yielded enamel cubes that could be more easily manipulated and weighted due to their larger sizes. In those instances, a fraction of the aliquot was measured for elemental concentrations of major elements (Ca, Mg, P, and Fe) and trace elements (REE, Sr, and Ba) on an inductively coupled plasma-atomic emission spectrometer (ICAP 6000 Series ICP spectrometer, Thermo Electron Corporation) for major elements and on an inductively coupled plasma-mass spectrometer (ICP-MS) (7500 Series ICP-MS, Agilent Technologies) for REE and other trace elements.

All samples were purified using three separate resins for chromatography to retrieve close to 100% of the calcium: AG 50WX-12 to remove matrix including phosphorus, AG 50W-X8 to remove iron, and Sr-specific resin to remove Sr. The reliability of elutions was controlled by processing and analyzing reference materials (NIST-SRM1486 and OSIL-IAPSO).

Calcium isotope abundance ratios ($^{44}Ca/^{42}Ca$) were measured using a Neptune Plus multicollector ICP-MS following Tacail et al. (2014). Following the purification step, all samples and reference materials were dried and re-dissolved in ultrapure nitric acid (0.05 N), and Ca concentrations were adjusted at 1.25 ppm. The Ca isotope compositions are expressed using the "delta" notation, which is defined as follows:

$$\delta^{44/42}Ca(‰) = (((^{44}Ca/^{42}Ca_{sample}) / (^{44}Ca/^{42}Ca_{ICP\ Ca\ Lyon}) - 1) * 1000 \quad (1)$$

where $(^{44}Ca/^{42}Ca)_{sample}$ and $(^{44}Ca/^{42}Ca)_{ICP\ Ca\ Lyon}$ are the Ca isotope abundance ratios measured in the tooth sample and the ICP Ca Lyon reference material, respectively. The ICP Ca Lyon reference material is a Specpure Ca plasma standard solution (Alfa Aesar) purified from Sr using Sr-Spec resin, and it is used as a bracketing reference material during Ca isotope measurements. NIST-SRM1486 and OSIL-IAPSO, which are respectively cow bone meal and seawater reference materials, were used as secondary reference materials to assess the accuracy of analytical procedures, including chemical purification. To ease comparison, all results are also expressed against SRM 915a (Table 1).

Assessment of Isotopic Data Accuracy

A set of procedural blanks was inserted during the purification sessions and did not exceed 100 ng of Ca. All samples fall on a mass-dependent line of 0.510 ± 0.014 (2 s.e), which agrees with the 0.5067 slope predicted by the linear approximation of exponential mass-dependent fractionation. The $\delta^{44/42}Ca$ values for NIST-SRM1486 are –0.96 ± 0.11‰ (2SD, n = 17, January 2019), –1.03 ± 0.06‰ (2SD, n = 9, March 2019), –0.99 ± 0.15‰ (2SD, n = 11, July 2019), and –1.00 ± 0.07‰ (2SD, n = 17, second session of July 2019). The seawater OSIL-IAPSO yielded values of +0.42 ± 0.05‰ (2SD, n = 2, March 2019) and +0.41 ± 0.04‰ (2SD, n = 4, July 2019). All of these standard values are within the range of previously published data from the ENS de Lyon Laboratory or from other works (Heuser and Eisenhauer, 2008; Heuser et al., 2011, 2016a, 2016b).

RESULTS

Raman Spectroscopy

Raman spectra obtained from dinosaur tooth enamel from the three geological formations are compared with a tooth enamel spectrum from a modern *Crocodylus niloticus* in Figure 2. A

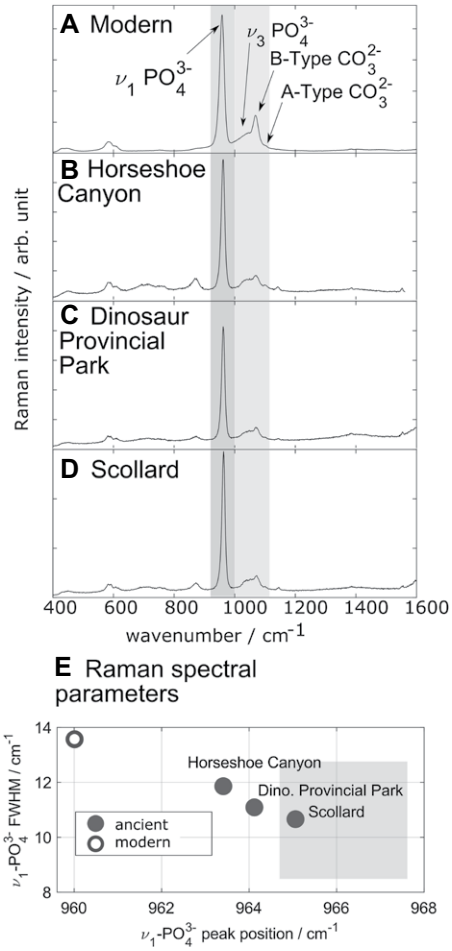

Figure 2. Comparison of modern versus fossil enamel UV Raman profiles from (A) a modern *Crocodylus niloticus*; (B) a hadrosaurid from the Horseshoe Canyon Formation; (C) a hadrosaurid from the Late Cretaceous Dinosaur Provincial Park Formation; and (D) a hadrosaurid from the Late Cretaceous Scollard Formation. Plotted along the *y*-axis are arbitrary units that are normalized relative to the $\nu 1\text{-}PO_4^{3-}$ peak. (E) Raman spectral parameters with $\nu 1\text{-}PO_4^{3-}$ full width at half maximum as a function of $\nu 1\text{-}PO_4^{3-}$ peak (in cm^{-1}) show the distribution of the modern and fossil enamel specimens in comparison to the alteration field (in gray) as defined by Thomas et al. (2011).

shift is detected in the strongest Raman peak of apatite ($\nu 1\text{-}PO_4^{3-}$) from 960 cm^{-1} in the modern enamel sample to 963–965 cm^{-1} in the three fossilized enamel samples (Figs. 2A–2D). The full width at half maximum (FWHM) of this peak is smaller in the fossil samples than in the modern one (Fig. 2E). The absence of a peak at 1080–1085 cm^{-1} precludes the presence of secondary carbonates.

TABLE 2. SUMMARY OF MAJOR, TRACE, AND REE (NORMALIZED TO NASC; GROMET ET AL., 1984) ELEMENTAL CONCENTRATIONS FOR A SUBSET OF SAMPLES ANALYZED IN THIS STUDY

Sample	Curation number	Tissue	Taxon	Formation	Ca (%)	P (%)	Ca/P	Mg (ppm)	Sr (ppm)	Ba (ppm)	$139La_N$	$140Ce_N$	$141Pr_N$
94.31.5den	TMP94.31.5	dentine	Tyrannosauridae	Scollard	33.73	14.17	2.38	646.02	1366.95	4202.44	2.70	2.72	5.00
JM59den	TMP1994.12.238	enamel	Ceratopsidae	Dinosaur Provincial Park	27.69	11.68	2.37	2066.96	1386.80	2712.16	21.83	26.52	40.41
94.31.5ena	TMP94.31.5	enamel	Tyrannosauridae	Scollard	91.36	38.64	2.36	1959.29	6682.38	15,667.20	63.49	61.87	109.07
96.040den	TMP1996.040.0004	dentine	Ceratopsidae	Horseshoe Canyon	11.70	5.18	2.26	158.07	251.01	398.67	0.79	0.83	1.53
jm62ena	TMP2011.012.0039	enamel	Tyrannosauridae	Dinosaur Provincial Park	35.21	15.60	2.26	914.13	854.79	1452.91	0.80	0.99	1.87
Sample (*continued*)	$146Nd_N$	$149Sm_N$	$153Eu_N$	$157Gd_N$	$159Tb_N$	$163Dy_N$	$165Ho_N$	$167Er_N$	$169Tm_N$	$171Yb_N$	$175Lu_N$	La/Sm_N	La/Yb_N
94.31.5den	6.43	9.14	9.27	15.37	11.99	-	17.91	19.15	16.79	19.86	17.84	0.30	0.14
JM59den	47.36	53.47	39.29	59.41	40.32	-	41.54	39.45	33.10	35.63	27.11	0.41	0.61
94.31.5ena	134.27	163.32	142.59	212.61	152.52	-	175.61	171.51	141.67	152.22	121.20	0.39	0.42
96.040den	1.92	2.54	2.45	3.64	2.70	-	3.17	3.10	2.67	2.99	2.58	0.31	0.26
jm62ena	2.17	2.88	2.12	3.31	2.64	-	2.78	2.66	2.58	2.74	2.23	0.28	0.29

Note: REE—rare earth element; NASC—North American shale composite.

Elemental Concentrations

Concentration analyses were run on a subset of samples because such analyses require a greater quantity of material than what is necessary for calcium isotopic analyses alone, and as explained above, one of the goals of the present study was to be as minimally destructive as possible. A first approach is to control for the modification of the calcium content of bioapatite by measuring its stoichiometry using Ca/P ratios. Here, Ca/P dinosaur tooth and dentine values (Table 2) agree with modern bioapatite values (Sillen, 1986) as well as results from a previous study on dinosaur tooth enamel (Hassler et al., 2018), which indicates that measured samples preserve the original stoichiometry of bioapatite.

Compared to the general REE composition of waters and sediments (data were normalized to the North American shale composite [NASC]; Gromet et al., 1984), both enamel and dentine bioapatite REE profiles from the Late Cretaceous of Canada are moderately enriched in light REE such as lanthanum and more enriched in intermediate (e.g., samarium) and heavy REE (e.g., ytterbium) (Fig. 3A), which is in line with terrestrial pore waters being enriched in heavy REE (Trueman and Tuross, 2002). Contrary to fossil samples having experienced important recrystallization processes (Reynard and Balter, 2014), none of the Canadian profiles are bell-shaped. La/Sm and La/Yb ratios inform about adsorption and/or substitution processes (e.g., Trueman and Tuross, 2002; Reynard and Balter, 2014). Here, both the enamel and dentine dinosaur samples fall within the range of modern freshwater samples (Fig. 3B), which supports the idea that these fossils experienced adsorption and substitutions processes of very moderate intensity.

Calcium Isotope Ratios

For the combined dinosaur tooth data set, dinosaur enamel $\delta^{44/42}$Ca values (expressed against the ICP Ca Lyon standard) range between –0.10‰ and –1.55‰ (Fig 4; Table 1). In all three formations, mean $\delta^{44/42}$Ca values of tyrannosaurid teeth are similar and are the most depleted of the data set (–1.03 ± 0.46‰, 2SD in the Scollard Formation; –1.11 ± 0.33‰, 2SD in the Horseshoe Canyon Formation; –1.13 ± 0.31‰, 2SD in the Dinosaur Park Formation). Ceratopsid $\delta^{44/42}$Ca values are slightly more ^{44}Ca-enriched than tyrannosaurid values in two of the formations (–0.93 ± 0.11‰, 2SD in the Scollard Formation; –0.68 ± 0.36‰, 2SD in the Horseshoe Canyon Formation) and widely overlap the distribution of tyrannosaurid $\delta^{44/42}$Ca values in the Dinosaur Park Formation (–1.05 ± 0.33‰, 2SD). Hadrosaurid $\delta^{44/42}$Ca values are the most ^{44}Ca-enriched group of the data set; they are significantly enriched compared to tyrannosaurid values and ~0.1–0.2‰ more enriched than ceratopsid $\delta^{44/42}$Ca values (–0.77‰ in the Scollard Formation; –0.61 ± 0.54‰, 2SD in the Horseshoe Canyon Formation; –0.68 ± 0.17‰, 2SD in the Dinosaur Park Formation). Nodosaurids and ankylosaurids are rare, and the few teeth analyzed from the Dinosaur Park Formation show $\delta^{44/42}$Ca values in the range of ceratopsids (–0.99 ± 0.11‰, 2SD for nodosaurids; –0.84 ± 0.18‰, 2SD for ankylosaurids). Calcium isotope values for most taxonomic groups are spread over a large isotopic range, which suggests variability in calcium source input, physiology, or both.

DISCUSSION

Dinosaur Bioapatite Alteration

Previous studies have reported calcium isotopic values for dinosaur dental tissues, providing evidence for minimal diagenetic impact on tooth enamel values (Heuser et al., 2011; Hassler et al., 2018), which is in line with previous studies that emphasized the hardness of enamel bioapatite (Lee-Thorp and van der Merwe, 1987; Ayliffe et al., 1994; Wang and Cerling, 1994). Due to the high concentration (above 30 wt%) of calcium in bioapatite, which contrasts strongly with the concentrations of trace metals (hundreds of ppm for Sr and lower than 100 ppm for Ba or Zn), and its strong binding in the lattice of bioapatite, this element may be viewed as immune to, or resistant against, important diagenetic alterations in sub-surface sedimentological contexts. In fact, only precipitates originating from highly isotopically fractionated fluids may substantially modify the original calcium isotopic composition, as modeled in Martin et al. (2017a). Such conditions would be readily met under metamorphic contexts where precipitation-solution mechanisms could affect bioapatite that is subjected to significant temperature and pressure (Reynard and Balter, 2014). Nevertheless, all three sedimentary formations underwent compaction and pore-fluid circulation during their post-burial history, and it is worth testing for any possible alteration of fossil bioapatite prior to isotopic measurements.

Major recrystallization processes seem unlikely in the sample set because bioapatite stoichiometry is preserved as evidenced by Ca/P ratios that are similar to modern bioapatite ratios (Sillen, 1986) and similar to those measured in a previous study of dinosaur tooth enamel (Hassler et al., 2018). Other types of evidence of recrystallization processes in dinosaur bioapatite can also be investigated by analyzing rare earth

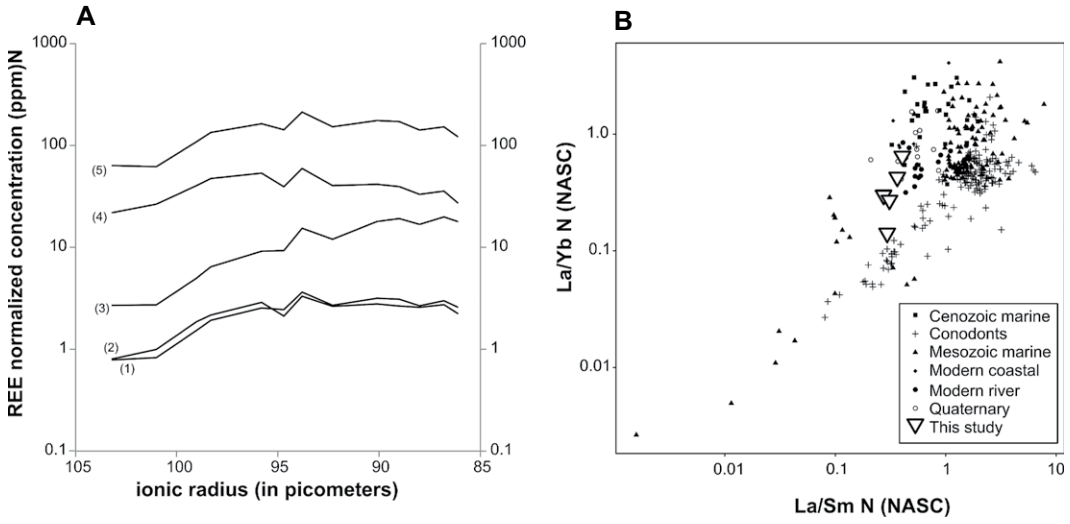

Figure 3. Trace element analyses of dinosaur bioapatite from the Late Cretaceous of Alberta, Canada, are shown. (A) Rare earth element (REE) patterns normalized to the North American shale composite (NASC) (Gromet et al., 1984) of dinosaur teeth including (1) dentine of a ceratopsid (TMP 1996.40.4) from the Horseshoe Canyon Formation, (2) enamel of a tyrannosaurid (TMP 2011.12.39) from the Dinosaur Park Formation, (3) dentine of a tyrannosaurid (TMP 1994.31.5) from the Scollard Formation, (4) dentine of a ceratopsid (TMP 1994.12.238) from the Dinosaur Park Formation, and (5) enamel of a tyrannosaurid (TMP 1994.31.5) from the Scollard Formation. (B) La/Sm_N as a function of La/Yb_N (normalized to NASC) for a variety of fossil bioapatite and modern waters (data from Reynard and Balter, 2014) with different diagenetic settings involving substitution and adsorption domains. The five enamel and dentine samples analyzed in this study fall within the domain of modern river waters.

elements (REEs). Because REEs are virtually absent from modern bioapatite and are incorporated into the lattice of bioapatite from the encasing sediment during burial (e.g., Trueman and Tuross, 2002), measuring REE in fossil bioapatite provides complementary information about their incorporation including depositional conditions and subsequent diagenetic history. The moderate enrichment in light REE with the more enriched profiles for intermediate and heavy REE observed in the tooth enamel samples indicate the inclusion of exogenous metals from the burial environment. However, the fact that none of the patterns are bell-shaped indicates that recrystallization processes were limited (Reynard and Balter, 2014). Adsorption and substitution processes took place and were of moderate intensity as indicated by the distribution of La/Sm and La/Yb ratios. Altogether, these data are consistent with a freshwater environment as the burial setting (Trueman and Tuross, 2002).

Because of their high calcium content, secondary carbonates are also a source of potential diagenetic alteration that may bias the calcium isotope values of original bioapatite. Heuser et al. (2011) have shown that dentine calcium isotopic values are systematically more enriched in ^{44}Ca than enamel values of the same modern reptile and dinosaur tooth sample, which suggests that the dentine-enamel Ca isotope difference observed in both dinosaur tissues may reflect a primary biological feature. Because dentine possesses canaliculi, it is slightly more porous than enamel and can accommodate tiny ($< 1\ \mu m$), secondary precipitates of calcium carbonate. However, the mass balance model of Heuser et al. (2011) indicates that pore infilling by secondary carbonates would barely shift the calcium isotope composition outside of analytical error. Although dentine, and possibly bone, are potential candidates for preservation of the primary biogenic Ca isotope values, apatite crystals do increase in size during fossilization, for example, through dissolution-reprecipitation of the primary apatite (see review in Trueman and Tuross, 2002). Dentine and bone may be important materials to measure, especially when facing the choice of including extinct edentulous taxa such as ornithomimosaurs, oviraptorosaurs, and therizinosaurs in paleoecological investigations. Beyond the present enamel Ca isotope data set, further investigation of dentine and bone, as initiated by Heuser et al. (2011), is desirable.

Thomas et al. (2007) have shown that Raman spectroscopy was a non-destructive and rapid technique for determining significant changes in the microcrystalline structure of biogenic phosphates (bones and teeth) induced by burial and fossilization processes (Olcott Marshall and Marshall, 2015; Keenan, 2016). As with other techniques, using Fourier-transform infrared spectroscopy and X-ray diffraction, Pucéat et al. (2004) defined a new crystallinity index from the ratio of the FWHM of the intense peak of the PO_4 symmetric stretching mode in a biogenic apatite sample. Measuring phosphate-oxygen isotopes ($\delta^{18}O_p$) in a wide range of modern and fossil, dentine, and enamel samples, Thomas et al. (2011) revealed a diagenetically altered field for the bioapatite, as defined within a diagram of Raman shift position and FWHM of the PO_4 symmetric stretching Raman mode (Fig. 2E). From Raman spectra, Dal Sasso et al. (2018) calculated parameters related to the collagen content, bioapatite crystallinity, and structural carbonate content as well as those related to the occurrence of secondary mineral phases. All of these studies have reinforced the ability of Raman spectroscopy to characterize the preservation state of ancient bioapatite. In the present study, deep UV Raman spectra were recorded for four enamel samples while staving off the luminescence generated by organics and REEs. Attempts to measure the Raman spectra of such samples with visible wavelength failed, and those were locally burned. The complete description of the Raman signatures collected is outside the scope of this study. The normalized raw Raman spectra of the enamel are plotted without data preprocessing. The Raman peak attributed to a secondary carbonate formation occurring after a diagenetic recrystallization of calcium compounds is not observed. This symmetric stretching mode of CO_3^{2-} vibration is expected around 1085 cm^{-1} in calcite and has a very strong Raman cross section. The FWHM and wavenumber position of the phosphate symmetric stretching mode ($\nu1\text{-}PO_4^{3-}$) are determined in three fossil enamel samples and in a modern archosaur enamel. Two zones can be highlighted in the spectra: the blue, centered on the $\nu1\text{-}PO_4^{3-}$ peak, and the red, centered on the mixed contribution of $\nu3\text{-}PO_4^{3-}$ and carbonate bands. The B and A types of $\nu1\text{-}CO_3^{2-}$ are 1070 cm^{-1} and 1098 cm^{-1}, respectively (Penel et al., 1998). The Raman spectral parameters plotted in Figure 2E are used as a proxy to assess the diagenetic alteration of the bioapatite. According to Thomas

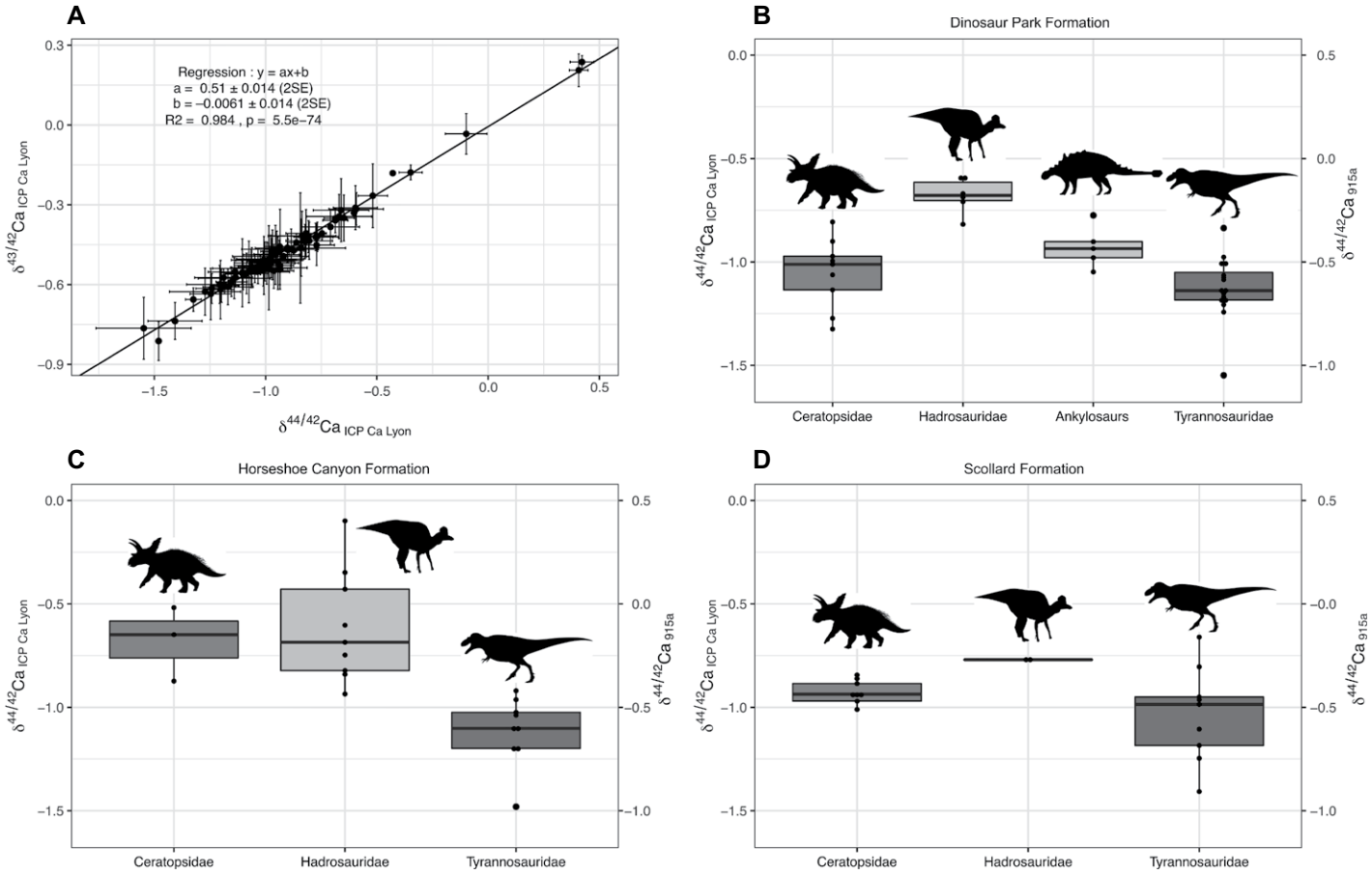

Figure 4. Calcium isotopic variability was recorded from tooth enamel of the three dinosaur assemblages analyzed in this work. (A) Mass-dependent fractionation line for all samples and standards analyzed in the present study (see Table 1); box and whisker plots show the distribution of $\delta^{44/42}$Ca values for herbivorous and tyrannosaurid dinosaurs in the (B) Dinosaur Park Formation; (C) Horseshoe Canyon Formation; and (D) Scollard Formation. The boxes represent the first and third quartiles with the medians as horizontal lines. The lower and upper whiskers represent 1.5× the interquartile range. Dinosaur silhouettes are from Phylopic.org.

et al. (2011), with a ν1-PO_4^{3-} peak position of 965 cm^{-1} and a FWHM of 10.7 cm^{-1}, the fossil enamel from the Scollard Formation plots in the diagenetic alteration field. Horseshoe Canyon and Dinosaur Provincial Park enamel specimens fall outside of this field.

Relevant to the study of Ca isotopes, detecting the presence of secondary carbonates from Raman spectra of the bioapatite crystals analyzed (Dal Sasso et al., 2018) is a useful complementary approach for assessing whether carbonate removal techniques (e.g., weak acid leaching) need to be conducted. Moreover, the deep UV approach allows for clear observation of the structural peaks of fossil bioapatite where other Raman measures in the range of visible light are often blurred by an elevated background from luminescent material incorporated during diagenesis (e.g., Thomas et al., 2007). Raman spectroscopic observations indicate that fossil bioapatite underwent structural alteration because a shift in the v1 band of apatite is detected in comparison to that of modern *Crocodylus* enamel. Structural carbonates occupy the same sites as structural phosphates, and if diagenesis is to be a concern for isotopic compositions of bioapatite, this may involve elements that constitute PO_4 and CO_3 such as C and O isotopes, but the extent of diagenetic impact on those isotopic systems is beyond the scope of the present study. Finally, as in the modern sample, there is no contribution of diagenetic calcium from secondary carbonates as indicated by the absence of a 1080–1085 cm^{-1} peak.

In summary, there is no evidence for alteration at the structural carbonate level in the dinosaur enamel bioapatite analyzed here. However, its chemical composition, except for the inclusion of trace metals as indicated by REE contents and patterns, does not include secondary carbonates and therefore should not include important amounts of exogenous calcium from the burial environment. Therefore, calcium isotope values measured from dinosaur enamel most likely reflect biogenic values.

Niche Partitioning Among Herbivores

Megaherbivorous dinosaurs were diverse during the Late Cretaceous in Alberta, Canada, with several species of hadrosaurids, ceratopsids, and ankylosaurs living in the same ecosystems. Although it is impossible to identify the preferred types of plants that formed the diet of the taxa studied, the calcium isotopic composition of teeth represents a mass-weighted isotopic average of the various plant items ingested. Thus, calcium isotopic data allow us to infer how variable dietary sources were within a given dinosaur ecosystem.

Previous studies have reported calcium isotope values for Jurassic and Cretaceous dinosaur assemblages where herbivorous dinosaurs displayed the most ^{44}Ca-enriched values (Heuser et al., 2011; Hassler et al., 2018), and this pattern

is confirmed in the present study. Hadrosaurids have similar isotopic values across the three Canadian rock formations and consistently display the most ^{44}Ca-enriched values of the data set, although this is less certain in the Scollard Formation due to the small (n = 2) sample size available. Hadrosaurid values (–0.65 ± 0.41‰, n = 17) are compatible with a previously published calcium isotopic value for a hadrosaurid from the Dinosaur Park Formation (Heuser et al., 2011) and comparable to iguanodontid values from the Aptian–Albian of Gadoufaoua, Niger (–0.56 ± 0.05‰, n = 9, Hassler et al., 2018). While different digestive physiologies cannot be ruled out, the calcium isotope data indicate that hadrosaurids fed on a ^{44}Ca-enriched plant source that was distinct from that of other sympatric megaherbivores in the Dinosaur Park Formation, where the distribution of calcium isotopic values between ceratopsids and hadrosaurids (Wilcoxon rank sum test, p-value = 0.0007) and between ankylosaurs and hadrosaurids (Wilcoxon rank sum test, p-value = 0.0086) is clearly distinct. This suggests that hadrosaurids did not forage on the same vegetation as ceratopsids and ankylosaurs in that formation. Indeed, biometric studies have shown that hadrosaurids were able to browse at both high and low levels, whereas ceratopsids and ankylosaurs could only feed on low foliage (Weishampel and Normal, 1989; Mallon et al., 2013; Mallon and Anderson, 2013). Because leaves from high vegetation tend to be more ^{44}Ca-enriched than lower-growing plant materials (Schmitt, 2016; Moynier and Fujii, 2017; Martin et al., 2018), the ^{44}Ca-enriched composition of hadrosaurid enamel supports the hypothesis that hadrosaurids foraged preferentially on tall plants, whereas the other megaherbivores fed on plants closer to the ground (Weishampel and Norman, 1989; see also Mallon et al., 2013). The aforementioned foraging flexibility of hadrosaurids could explain the isotopic signature overlaps occasionally observed among this clade and other megaherbivores.

Ceratopsid values from the Dinosaur Park and Scollard formations overlap with tyrannosaurid values and are slightly more positive. In contrast, ceratopsid values are distinctly ^{44}Ca-enriched relative to tyrannosaurid values in the Horseshoe Canyon Formation. Ceratopsids differ significantly from Hadrosauridae in their more ^{44}Ca-depleted values in the Dinosaur Park Formation, but overlap with hadrosaurids in the Horseshoe Canyon Formation. Ceratopsid teeth from the Dinosaur Park and Horseshoe Canyon formations display a greater range of calcium isotope values than those from the Scollard Formation. This spread in data could be due to the higher diversity of ceratopsids known from the former formations (at least six ceratopsids in the Dinosaur Park Formation and at least three in the Horseshoe Canyon Formation) compared to the Scollard Formation, where *Triceratops* is the only ceratopsid known (Mallon et al., 2012; Eberth et al., 2013; Eberth and Kamo, 2020). As such, the ceratopsid teeth from the Dinosaur Park and Horseshoe Canyon Formations may sample a greater range of dietary preferences or, as they come from a longer time interval, a greater range of paleoenvironmental settings than those from the Scollard Formation.

Ankylosaur teeth are less common than those of hadrosaurids and ceratopsids and, as such, are represented in the data set only for the Dinosaur Park Formation. Although previous studies have suggested that ankylosaurids and nodosaurids possibly had different dietary preferences, with one clade feeding on tougher vegetation than the other (Rybczynski and Vickaryous, 2001; Mallon and Anderson, 2013), the calcium isotopic values for these two clades cannot be distinguished from each other or from those of ceratopsids. These results are consistent with previous studies indicating that these megaherbivores were limited to feeding on low vegetation (Bakker, 1978; Weishampel and Norman, 1989; Vickaryous et al., 2004; Mallon et al., 2013; Mallon and Anderson, 2013), although the limited sample size precludes detection of potential dietary preferences and invites further study of this taxonomic group.

The differences in calcium isotopic values observed among megaherbivorous dinosaurs may reflect dietary differences in ingested plant types. In modern mammalian ecosystems, grazers tend to show ^{44}Ca-depleted values relative to browsers, which can be explained by differences in either plant type or plant organs ingested or in digestive physiology (Martin et al., 2018). It has been inferred, based on isotopic evidence, that hadrosaurids preferentially frequented forested settings whereas ceratopsids alternatively frequented open and understory forests at various times (Fricke and Pearson, 2008), and this result is also in agreement with other approaches (Brinkman et al., 1998; Cullen and Evans, 2016; Oreska and Carrano, 2019). As such, it is possible that these different habitat preferences of hadrosaurids and ceratopsids could be the source of the calcium isotopic differences between the two clades in the Dinosaur Park Formation. In contrast, the similarity of calcium isotopic signatures between hadrosaurids and ceratopsids in the Horseshoe Canyon Formation suggests these megaherbivores fed on similar plant resources and/or frequented similar habitats, as opposed to their dietary or ecological segregation in the Dinosaur Park Formation. Comparing isotopic values from different megaherbivore clades collected within a finer stratigraphic resolution (i.e., closer to isochronous) may yield important results for understanding the evolution of trophic dynamics.

The results of the present study also offer insight into the "sauropod hiatus" in North America, a time interval during the Late Cretaceous when sauropod dinosaurs were absent while they remained abundant elsewhere in the world, especially in regions that were formerly part of Gondwana (Lucas and Hunt, 1989; Mannion and Upchurch, 2011). Here, hadrosaurid calcium isotope values from Alberta are within the range of ^{44}Ca-enriched values of sauropod dinosaurs from the Upper Jurassic of Tendaguru, Tanzania, the Late Jurassic Morrison Formation, USA (Heuser et al., 2011), and the Cretaceous of Gadoufaoua in Niger (Hassler et al., 2018), which all display among the most ^{44}Ca-enriched values for herbivorous dinosaurs in the literature. Calcium isotopic differences in geological substrates range between ~0‰ for silicates and ~–0.2‰ for carbonates (Tipper et al., 2016) and, for this reason, their isotopic imprint on the food web (routed through plant root uptake or drinking water) appears smaller than differences that are due to the trophic level effect. With this in mind, the similarity in $\delta^{44/42}$Ca values of hadrosaurid and sauropod teeth suggests that the two clades fed on comparable plant resources, which is indicative that both groups fed on tall plants. This raises the possibility that hadrosaurids filled the ecological niches left vacant by the disappearance of sauropods in North America during the Late Cretaceous. Testing niche partitioning or overlap between Late Cretaceous hadrosaurids and sauropods could be achieved by analyzing specimens that mark the end of the "sauropod hiatus" in the southern USA, i.e., from the Maastrichtian deposits of the Ojo Alamo Formation in New Mexico and the Javelina Formation in Texas, where both groups have been reported to coexist (e.g., Lehman et al., 2016; Williamson and Weil, 2008).

Tyrannosaurid Feeding Preferences

Tyrannosaurids are the archetypal predatory dinosaurs in popular culture and, although a wealth of information is known about these animals (see Brusatte et al., 2010), many uncertainties and much speculation remain with regards to their dietary habits. The results of this study offer a different perspective on diet, where calcium isotope values of tyrannosaurid teeth reflect the average values of various dietary sources ingested in different proportions. Although some values are extremely low and may reflect bone ingestion (Heuser et al., 2011), all tyrannosaurid teeth from the three formations display comparably wide ranges

of calcium isotope values, which can be interpreted as the result of opportunistic feeding behavior on a wide diversity of prey. The fact that no distinct isotopic change is observed in tyrannosaurids through the Campanian–Maastrichtian time interval suggests access to a wide spectrum of available prey resources, at least at the chronological resolution available here (i.e., based on museum specimens collected at different levels of the three formations). A puzzling aspect is the presence of two ^{44}Ca-enriched tyrannosaurid teeth from the Scollard Formation (i.e., more positive than –0.8‰). Diagenetic alteration of tooth enamel driving the isotopic values toward more positive values cannot be completely dismissed because the sampling strategy was not devised to monitor diagenesis of all individual teeth in the data set. Another possible explanation may be a ^{44}Ca-enriched terrestrial prey source, such as a particularly ^{44}Ca-enriched hadrosaurid or ceratopsid prey source. A direct validation of this hypothesis is, however, hampered by the few available hadrosaurid specimens from the Scollard Formation, where only two individuals were analyzed. Some hadrosaurids from the underlying Horseshoe Canyon Formation are ^{44}Ca-enriched and match the expectation of such a potential prey source for the few tyrannosaurids with relatively high Ca isotope values. Further investigation of the hadrosaurid-tyrannosaurid trophic relationship during the late Maastrichtian should be explored in the time-equivalent Hell Creek Formation, where hadrosaurids may be more available for sampling. A less likely possibility for the two tyrannosaurid outliers is that a marine food source drove the enamel Ca isotope values toward the ^{44}Ca-enriched seawater endmember (+0.41‰) (Skulan et al., 1997). Whereas there is no evidence of marine influence in the Scollard Formation (Eberth and O'Connell, 1995), it has been positively identified in the contemporaneous Hell Creek Formation of southern North Dakota (Murphy et al., 2002) and in the Frenchman Formation of southern Saskatchewan (Cockx et al., 2021), which are more than 900 km and 450 km away, respectively. As one of the largest land predators to have existed, *T. rex* may have roamed large distances, and proximity of the Western Interior Seaway may have afforded occasional dietary supplement of stranded marine animals, including carcasses of plesiosaurs, mosasaurs, and fishes, to the more traditional terrestrial menu. On the other hand, the Bearpaw Sea was closer to terrestrial ecosystems of the upper part of Dinosaur Park and the lower part of the Horseshoe Canyon Formation, so any record of seafood diet is more likely to be preserved in the carnivorous species inhabiting these ecosystems. Evaluating the hypothesis of terrestrial versus seafood consumption in tyrannosaurids further requires joint spatial measurements of calcium and radiogenic strontium isotopes in *Albertosaurus*, *Daspletosaurus*, and *Gorgosaurus* teeth with monitoring of tooth enamel diagenetic alteration.

Tyrannosaurid median calcium isotope values overlap with ceratopsid values from the Dinosaur Park Formation (Wilcoxon rank sum test, p-value = 0.2071) and from the Scollard Formation (Wilcoxon rank sum test, p-value = 0.1672) but not from the Horseshoe Canyon Formation (Wilcoxon rank sum test, p-value = 0.0090). Tyrannosaurid values are, however, lower than hadrosaurid values in all three formations (Wilcoxon rank sum test, p-value = 4.322e-10). The mean difference between tyrannosaurid and hadrosaurid enamel $\delta^{44/42}$Ca values is -0.45‰ in the Dinosaur Park Formation and -0.50‰ in the Horseshoe Canyon Formation, which is close to the -0.57‰ offset commonly reported between the diet and bones of modern animals (e.g., Skulan and DePaolo, 1999; Tacail et al., 2020). Here, Ca isotope results suggest that tyrannosaurids from the Dinosaur Park Formation had a prey preference for hadrosaurids, a predator-prey relationship previously discussed in light of exploratory nitrogen isotope analyses (Ostrom et al., 1993), although it should be noted that the δ^{15}N values of ceratopsids and hadrosaurids overlap within 1SD. Such a predator–prey relationship is compatible with the greater abundance of tooth marks observed on hadrosaurid bones than on ceratopsid bones in that formation (Jacobsen, 1998) as well as fossil specimens representing instantaneous theropod feeding evidence, such as a partial hadrosaurid carcass associated with shed tyrannosaurid teeth (Currie, 1980) or a *Daspletosaurus* specimen preserving juvenile hadrosaurid bones that are interpreted as stomach content (Varricchio, 2001). However, the presence of numerous, laterally extensive (hundred meter to kilometer scale), monogeneric ceratopsid bonebeds in the Dinosaur Park Formation indicate that ceratopsid carcasses may have been occasionally abundant during mass mortality events (i.e., coastal floods resulting in mass drownings; Eberth and Getty, 2005). Under such circumstances, ceratopsids would have been abundantly available to scavengers such as tyrannosaurids, but only for a relatively limited amount of time. Considering the diet-bone offset of -0.57‰, the core of the tyrannosaurid Ca isotope data set does not indicate a prey preference for ceratopsids in the Dinosaur Park Formation. However, tyrannosaurids from the Horseshoe Canyon Formation and a few tyrannosaurid outliers with ^{44}Ca-depleted values from the Dinosaur Park and Scollard formations may represent individuals that fed on ceratopsids.

Tyrannosaurids are also known to have fed on other theropods, including conspecifics, as indicated by tooth marks on theropod bones from the Dinosaur Park Formation (Jacobsen, 1998). Because predators, by virtue of their diet, represent a ^{44}Ca-depleted dietary source, the few ^{44}Ca-depleted tyrannosaurid values in the data set could also reflect feeding on conspecifics, although it is impossible to distinguish this possibility from feeding on ceratopsid prey, which have overlapping calcium isotopic signatures in the Dinosaur Park and Scollard formations. Other sympatric theropods (e.g., dromaeosaurids and ornithomimids) are potential prey but have not been the subjects of analysis yet.

CONCLUSIONS

This study identified calcium isotope variability in tooth enamel of dinosaurs from the Late Cretaceous of North America and, when sample size was sufficiently large, statistically significant differences between taxonomic groups, which are interpreted here to reflect the dietary preferences of both megaherbivores and carnivores. New isotopic proxies, such as Ca isotopes, could contribute to a better understanding of how trophic guilds evolved and the stability of dinosaur communities in the millions of years preceding the end of the Cretaceous (Sakamoto et al., 2016; Chiarenza et al., 2019; Bonsor et al., 2020).

In the three uppermost Cretaceous sedimentary formations of Alberta, Canada, dinosaur enamel $\delta^{44/42}$Ca values display systematic, diet-related inter-taxon differences and provide encouragement for the study of isotopic variability at the individual scale to evaluate ecological behaviors linked to spatial or seasonal variations in diet or habitat partitioning (Fricke and Pearson, 2008), mobility (Terrill et al., 2020), and ontogenetic dietary shifts (Woodward et al., 2020; Therrien et al., 2021). With Ca isotope procedures allowing high-precision and high-resolution sampling, such questions may easily be investigated using this method. Moreover, considering the particularly minor damage to specimens that Ca isotope analysis entails, analyzing rare and unique specimens may be envisioned.

ACKNOWLEDGMENTS

J.E. Martin thanks D. Henderson for help and support during his visit to Royal Tyrrell Museum of Palaeontology (RTMP), Drumheller, Alberta, Canada, and Dinosaur Provincial Park as well as D.B. Brinkman and B. Strilisky at RTMP for facilitating access to the collections. We thank F. Arnaud-Godet and P. Télouk for assistance with the concentration and isotopic analyses, B. Reynard for sharing the data set used in

Figure 1B, and S. Martin for providing the *Crocodylus* tooth from la Ferme aux Crocodiles, Pierrelatte, France, used for the Raman analysis. The dinosaur outlines in Figures 1 and 4 were retrieved from www.phylopic.org and were contributed by A. Farke, E. Willoughby, C. Dylke, M. Ruiz-Villareal, and M. Dempsey. We thank them for transferring their work to the public domain or through a creative commons license. Geochemical analyses conducted in this work were partly supported by the Agence Nationale de la Recherche (SEBEK project no. ANR-19-CE31-0006-01 to J.E. Martin), by the Centre National de la Recherche Scientifique, Institut National des Sciences de l'Univers (CNRS INSU), and by École Normale Supérieure de Lyon (ENS Lyon), Lyon, France. RTMP provided authorization for specimen sampling and supported fieldwork at Dinosaur Provincial Park. The final version of this work benefited from the comments of Editor R. Strachan, Associate Editor B. Pratt, as well as two anonymous reviewers.

REFERENCES CITED

Amiot, R., Wang, X., Zhou, Z., Wang, X., Lécuyer, C., Buffetaut, E., Fluteau, F., Ding, Z., Kusuhashi, N., Mo, J., and Philippe, M., 2015, Environment and ecology of East Asian dinosaurs during the Early Cretaceous inferred from stable oxygen and carbon isotopes in apatite: Journal of Asian Earth Sciences, v. 98, p. 358–370, https://doi.org/10.1016/j.jseaes.2014.11.032.

Ayliffe, L.K., Chivas, A.R., and Leakey, M.G., 1994, The retention of primary oxygen isotope compositions of fossil elephant skeletal phosphate: Geochimica et Cosmochimica Acta, v. 58, p. 5291–5298, https://doi.org/10.1016/0016-7037(94)90312-3.

Bakker, R.T., 1978, Dinosaur feeding behaviour and the origin of flowering plants: Nature, v. 274, p. 661–663, https://doi.org/10.1038/274661a0.

Bonsor, J.A., Barrett, P.M., Raven, T.J., and Cooper, N., 2020, Dinosaur diversification rates were not in decline prior to the K–Pg boundary: Royal Society Open Science, v. 7, https://doi.org/10.1098/rsos.201195.

Bourgon, N., Jaouen, K., Bacon, A.M., Jochum, K.P., Dufour, E., Duringer, P., Ponche, J.L., Joannes-Boyau, R., Boesch, Q., Antoine, P.O., Hullot, M., Weis, U., Schulz-Kornas, E., Trost, M., Fiorillo, D., Demeter, F., Patole-Edoumba, E., Shackelford, L.L., Dunn, T.L., Zachwieja, A., Duangthongchit, S., Sayavonkhamdy, T., Sichanthongtip, P., Sihanam, D., Souksavatdy, V., Hublin, J.-J., and Tütken, T., 2020, Zinc isotopes in Late Pleistocene fossil teeth from a Southeast Asian cave setting preserve paleodietary information: Proceedings of the National Academy of Sciences of the United States of America, v. 117, p. 4675–4681, https://doi.org/10.1073/pnas.1911744117.

Brinkman, D.B., Ryan, M.J., and Eberth, D.A., 1998, The paleogeographic and stratigraphic distribution of ceratopsids (Ornithischia) in the upper Judith River Group of Western Canada: Palaios, v. 13, p. 160–169, https://doi.org/10.2307/3515487.

Brusatte, S.L., Norell, M.A., Carr, T.D., Erickson, G.M., Hutchinson, J.R., Balanoff, A.M., Bever, G.S., Choiniere, J.N., Makovicky, P.J., and Xu, X., 2010, Tyrannosaur paleobiology: New research on ancient exemplar organisms: Science, v. 329, p. 1481–1485, https://doi.org/10.1126/science.1193304.

Cant, D., and Stockmal, G., 1989, The Alberta foreland basin: Relationship between stratigraphy and Cordilleran terrane-accretion events: Canadian Journal of Earth Sciences, v. 26, p. 1964–1975, https://doi.org/10.1139/e89-166.

Catuneanu, O., Sweet, A.R., and Miall, A.D., 2000, Reciprocal stratigraphy of the Campanian–Paleocene Western Interior of North America: Sedimentary Geology, v. 134, p. 235–255, https://doi.org/10.1016/S0037-0738(00)00045-2.

Cerling, T.E., Hart, J.A., and Hart, T.B., 2004, Stable isotope ecology in the Ituri Forest: Oecologia, v. 138, p. 5–12, https://doi.org/10.1007/s00442-003-1375-4.

Chiarenza, A.A., Mannion, P.D., Lunt, D.J., Farnsworth, A., Jones, L.A., Kelland, S.J., and Allison, P.A., 2019, Ecological niche modelling does not support climatically-driven dinosaur diversity decline before the Cretaceous/Paleogene mass extinction: Nature Communications, v. 10, p. 1–14, https://doi.org/10.1038/s41467-019-08997-2.

Chu, N.-C., Henderson, G.M., Belshaw, N.S., and Hedges, R.E.M., 2006, Establishing the potential of Ca isotopes as proxy for consumption of dairy products: Applied Geochemistry, v. 21, p. 1656–1667, https://doi.org/10.1016/j.apgeochem.2006.07.003.

Clementz, M.T., Holden, P., and Koch, P.L., 2003, Are calcium isotopes a reliable monitor of trophic level in marine settings?: International Journal of Osteoarchaeology, v. 13, p. 29–36, https://doi.org/10.1002/oa.657.

Cockx, P., Tappert, R., Muehlenbachs, K., Somers, C., and McKellar, R.C., 2021, Amber from a *Tyrannosaurus rex* bonebed (Saskatchewan, Canada) with implications for paleoenvironment and paleoecology: Cretaceous Research, v. 125, https://doi.org/10.1016/j.cretres.2021.104865.

Cullen, T.M., and Evans, D.C., 2016, Palaeoenvironmental drivers of vertebrate community composition in the Belly River Group (Campanian) of Alberta, Canada, with implications for dinosaur biogeography: BMC Ecology, v. 16, article no. 52, https://doi.org/10.1186/s12898-016-0106-8.

Cullen, T.M., Longstaffe, F.J., Wortmann, U.G., Huang, L., Fanti, F., Goodwin, M.B., Ryan, M.J., and Evans, D.C., 2020, Large-scale stable isotope characterization of a Late Cretaceous dinosaur-dominated ecosystem: Geology, v. 48, p. 546–551, https://doi.org/10.1130/G47399.1.

Currie, P.J., 1980, Mesozoic vertebrate life in Alberta and British Columbia: Mesozoic Vertebrate Life, v. 1, p. 27–40.

Currie, P.J., Langston, W., and Tanke, D.H., 2008, A New Horned Dinosaur from an Upper Cretaceous Bonebed in Alberta: Ottawa, Ontario, Canada, NRC Research Press, 152 p., https://doi.org/10.1139/9780660198194.

Dal Sasso, G., Angelini, I., Maritan, L., and Artioli, G., 2018, Raman hyperspectral imaging as an effective and highly informative tool to study the diagenetic alteration of fossil bones: Talanta, v. 179, p. 167–176, https://doi.org/10.1016/j.talanta.2017.10.059.

D'Emic, M.D., O'Connor, P.M., Pascucci, T.R., Gavras, J.N., Mardakhayava, E., and Lund, E.K., 2019, Evolution of high tooth replacement rates in theropod dinosaurs: PLoS ONE, v. 14, https://doi.org/10.1371.journal.pone.0224734.

DeNiro, M.J., and Epstein, S., 1978, Influence of diet on the distribution of carbon isotopes in animals: Geochimica et Cosmochimica Acta, v. 42, p. 495–506, https://doi.org/10.1016/0016-7037(78)90199-0.

Eberth, D., 2005, The geology, *in* Currie, P.J., and Koppelhus, E., eds., Dinosaur Provincial Park, a Spectacular Ancient Ecosystem Revealed: Bloomington and Indianapolis, Indiana, Indiana University Press, p. 312–348.

Eberth, D., and Getty, M.A., 2005, Ceratopsian bonebeds: Occurrence, origins, and significance, *in* Currie, P.J., and Koppelhus, E., eds., Dinosaur Provincial Park, a Spectacular Ancient Ecosystem Revealed: Bloomington and Indianapolis, Indiana, Indiana University Press, p. 501–536.

Eberth, D.A., and Braman, D.R., 2012, A revised stratigraphy and depositional history for the Horseshoe Canyon Formation (Upper Cretaceous), southern Alberta plains: Canadian Journal of Earth Sciences, v. 49, p. 1053–1086, https://doi.org/10.1139/e2012-035.

Eberth, D.A., and Kamo, S.L., 2019, First high-precision U–Pb CA–ID–TIMS age for the Battle Formation (Upper Cretaceous), Red Deer River valley, Alberta, Canada: Implications for ages, correlations, and dinosaur biostratigraphy of the Scollard, Frenchman, and Hell Creek formations: Canadian Journal of Earth Sciences, v. 56, p. 1041–1051, https://doi.org/10.1139/cjes-2018-0098.

Eberth, D.A., and Kamo, S.L., 2020, High-precision U–Pb CA–ID–TIMS dating and chronostratigraphy of the dinosaur-rich Horseshoe Canyon Formation (Upper Cretaceous, Campanian–Maastrichtian), Red Deer River valley, Alberta, Canada: Canadian Journal of Earth Sciences, v. 57, p. 1220–1237, https://doi.org/10.1139/cjes-2019-0019.

Eberth, D.A., and O'Connell, S.C., 1995, Notes on changing paleoenvironments across the Cretaceous-Tertiary boundary (Scollard Formation) in the Red Deer River valley of southern Alberta: Bulletin of Canadian Petroleum Geology, v. 43, no. 1, p. 44–53.

Eberth, D.A., Evans, D.C., Brinkman, D.B., Therrien, F., Tanke, D.H., and Russell, L.S., 2013, Dinosaur biostratigraphy of the Edmonton Group (Upper Cretaceous), Alberta, Canada: evidence for climate influence: Canadian Journal of Earth Sciences, v. 50, no. 7, p. 701–726, https://doi.org/10.1139/cjes-2012-0185.

Erickson, G.M., 1996, Incremental lines of von Ebner in dinosaurs and the assessment of tooth replacement rates using growth line counts: Proceedings of the National Academy of Sciences of the United States of America, v. 93, p. 14623–14627, https://doi.org/10.1073/pnas.93.25.14623.

Erickson, G.M., Krick, B.A., Hamilton, M., Bourne, G.R., Norell, M.A., Lilleodden, E., and Sawyer, W.G., 2012, Complex dental structure and wear biomechanics in hadrosaurid dinosaurs: Science, v. 338, p. 98–101, https://doi.org/10.1126/science.1224495.

Erickson, G.M., Sidebottom, M.A., Kay, D.I., Turner, K.T., Ip, N., Norell, M.A., Sawyer, W.G., and Krick, B.A., 2015, Wear biomechanics in the slicing dentition of the giant horned dinosaur *Triceratops*: Science Advances, v. 1, https://doi.org/10.1126/sciadv.1500055.

Frederickson, J.A., Engel, M.H., and Cifelli, R.L., 2018, Niche partitioning in Theropod Dinosaurs: Diet and habitat preference in predators from the Uppermost Cedar Mountain Formation (Utah, USA): Scientific Reports, v. 8, p. 1–13, https://doi.org/10.1038/s41598-018-35689-6.

Fricke, H.C., and Pearson, D.A., 2008, Stable isotope evidence for changes in dietary niche partitioning among hadrosaurian and ceratopsian dinosaurs of the Hell Creek Formation, North Dakota: Paleobiology, v. 34, p. 534–552, https://doi.org/10.1666/08020.1.

Fricke, H.C., Rogers, R.R., Backlund, R., Dwyer, C.N., and Echt, S., 2008, Preservation of primary stable isotope signals in dinosaur remains, and environmental gradients of the Late Cretaceous of Montana and Alberta: Palaeogeography, Palaeoclimatology, Palaeoecology, v. 266, p. 13–27, https://doi.org/10.1016/j.palaeo.2008.03.030.

Fricke, H.C., Rogers, R.R., and Gates, T.A., 2009, Hadrosaurid migration: Inferences based on stable isotope comparisons among Late Cretaceous dinosaur localities: Paleobiology, v. 35, p. 270–288, https://doi.org/10.1666/08025.1.

Gromet, L.P., Dymek, R.F., Haskin, L.A., and Korotev, R.L., 1984, The "North American shale composite": Its compilation, major and trace element characteristics: Geochimica et Cosmochimica Acta, v. 48, p. 2469–2482, https://doi.org/10.1016/0016-7037(84)90298-9.

Hassler, A., Martin, J.E., Amiot, R., Tacail, T., Arnaud Godet, F., Allain, R., and Balter, V., 2018, Calcium isotopes offer clues on resource partitioning among Cretaceous predatory dinosaurs: Proceedings of the Royal Society B: Biological Sciences, v. 285, https://doi.org/10.1098/rspb.2018.0197.

Heuser, A., and Eisenhauer, A., 2008, The calcium isotope composition ($\delta^{44/40}$Ca) of NIST SRM 915b and NIST SRM 1486: Geostandards and Geoanalytical Research, v. 32, p. 311–315, https://doi.org/10.1111/j.1751-908X.2008.00877.x.

Heuser, A., Tütken, T., Gussone, N., and Galer, S.J., 2011, Calcium isotopes in fossil bones and teeth—Diagenetic versus biogenic origin: Geochimica et Cosmochimica Acta, v. 75, p. 3419–3433, https://doi.org/10.1016/j.gca.2011.03.032.

Heuser, A., Eisenhauer, A., Scholz-Ahrens, K.E., and Schrezenmeir, J., 2016a, Biological fractionation of stable Ca isotopes in Göttingen minipigs as a physiological model for Ca homeostasis in humans: Isotopes in Environmental and Health Studies, v. 52, p. 633–648, https://doi.org/10.1080/10256016.2016.1151017.

Heuser, A., Schmitt, A., Gussone, N., and Wombacher, F., 2016b, Analytical methods, *in* Gussone, N., et al., eds.,

Calcium Stable Isotope Geochemistry: Berlin, Heidelberg, Germany, Springer, p. 23–73, https://doi.org/10.1007/978-3-540-68953-9_2.

Jacobsen, A.R., 1998, Feeding behaviour of carnivorous dinosaurs as determined by tooth marks on dinosaur bones: Historical Biology, v. 13, p. 17–26, https://doi.org/10.1080/08912969809386569.

Jaouen, K., Beasley, M., Schoeninger, M., Hublin, J.J., and Richards, M.P., 2016, Zinc isotope ratios of bones and teeth as new dietary indicators: Results from a modern food web (Koobi Fora, Kenya): Scientific Reports, v. 6, p. 1–8, https://doi.org/10.1038/srep26281.

Keenan, S.W., 2016, From bone to fossil: A review of the diagenesis of bioapatite: The American Mineralogist, v. 101, no. 9, p. 1943–1951, https://doi.org/10.2138/am-2016-5737.

Kohn, M.J., Schoeninger, M.J., and Valley, J.W., 1996, Herbivore tooth oxygen isotope compositions: Effects of diet and physiology: Geochimica et Cosmochimica Acta, v. 60, p. 3889–3896, https://doi.org/10.1016/0016-7037(96)00248-7.

Kohn, M.J., Schoeninger, M.J., and Barker, W.W., 1999, Altered states: Effects of diagenesis on fossil tooth chemistry: Geochimica et Cosmochimica Acta, v. 63, p. 2737–2747, https://doi.org/10.1016/S0016-7037(99)00208-2.

Kohn, M.J., Morris, J., and Olin, P., 2013, Trace element concentrations in teeth–a modern Idaho baseline with implications for archeometry, forensics, and palaeontology: Journal of Archaeological Science, v. 40, p. 1689–1699, https://doi.org/10.1016/j.jas.2012.11.012.

Lee-Thorp, J.A., and van der Merwe, N.J., 1987, Carbon isotope analysis of fossil bone apatite: South African Journal of Science, v. 83, p. 712–715.

Lehman, T.M., Wick, S.L., and Wagner, J.R., 2016, Hadrosaurian dinosaurs from the Maastrichtian Javelina Formation, Big Bend National Park, Texas: Journal of Paleontology, v. 90, p. 333–356, https://doi.org/10.1017/jpa.2016.48.

Leichliter, J.N., Lüdecke, T., Foreman, A.D., Duprey, N.N., Winkler, D.E., Kast, E.R., Vonhof, H., Sigman, D.M., Haug, G.H., Clauss, M., Tütken, T., and Martínez-García, A., 2020, Nitrogen isotopes in tooth enamel record diet and trophic level enrichment: Results from a controlled feeding experiment: Chemical Geology, v. 563, https://doi.org/10.1016/j.chemgeo.2020.120047.

Lucas, S.G., and Hunt, A.P., 1989, *Alamosaurus* and the sauropod hiatus in the Cretaceous of the North American Western Interior, *in* Farlow, J.O., ed., Paleobiology of the Dinosaurs: Boulder, Colorado, Geological Society of America Special Paper 238, p. 75–85, https://doi.org/10.1130/SPE238-p75.

Mallon, J.C., and Anderson, J.S., 2013, Skull ecomorphology of megaherbivorous dinosaurs from the Dinosaur Park Formation (upper Campanian) of Alberta, Canada: PLoS One, v. 8, https://doi.org/10.1371/journal.pone.0067182.

Mallon, J.C., and Anderson, J.S., 2014, The functional and palaeoecological implications of tooth morphology and wear for the megaherbivorous dinosaurs from the Dinosaur Park Formation (upper Campanian) of Alberta, Canada: PLoS One, v. 9, https://doi.org/10.1371/journal.pone.0098605.

Mallon, J.C., Evans, D.C., Ryan, M.J., and Anderson, J.S., 2012, Megaherbivorous dinosaur turnover in the Dinosaur Park Formation (upper Campanian) of Alberta, Canada: Palaeogeography, Palaeoclimatology, Palaeoecology, v. 350, p. 124–138, https://doi.org/10.1016/j.palaeo.2012.06.024.

Mallon, J.C., Evans, D.C., Ryan, M.J., and Anderson, J.S., 2013, Feeding height stratification among the herbivorous dinosaurs from the Dinosaur Park Formation (upper Campanian) of Alberta, Canada: BMC Ecology, v. 13, p. 14, https://doi.org/10.1186/1472-6785-13-14.

Mannion, P.D., and Upchurch, P., 2011, A re-evaluation of the 'mid-Cretaceous sauropod hiatus' and the impact of uneven sampling of the fossil record on patterns of regional dinosaur extinction: Palaeogeography, Palaeoclimatology, Palaeoecology, v. 299, no. 3–4, p. 529–540, https://doi.org/10.1016/j.palaeo.2010.12.003.

Martin, J.E., Tacail, T., Adnet, S., Girard, C., and Balter, V., 2015, Calcium isotopes reveal the trophic position of extant and fossil elasmobranchs: Chemical Geology, v. 415, p. 118–125, https://doi.org/10.1016/j.chemgeo.2015.09.011.

Martin, J.E., Tacail, T., and Balter, V., 2017a, Non-traditional isotope perspectives in vertebrate palaeobiology: Palaeontology, v. 60, p. 485–502, https://doi.org/10.1111/pala.12300.

Martin, J.E., Vincent, P., Tacail, T., Khaldoune, F., Jourani, E., Bardet, N., and Balter, V., 2017b, Calcium isotopic evidence for vulnerable marine ecosystem structure prior to the K/Pg extinction: Current Biology, v. 27, p. 1641–1644, https://doi.org/10.1016/j.cub.2017.04.043.

Martin, J.E., Tacail, T., Cerling, T.E., and Balter, V., 2018, Calcium isotopes in enamel of modern and Plio-Pleistocene East African mammals: Earth and Planetary Science Letters, v. 503, p. 227–235, https://doi.org/10.1016/j.epsl.2018.09.026.

Mitchell, J.S., Roopnarine, P.D., and Angielczyk, K.D., 2012, Late Cretaceous restructuring of terrestrial communities facilitated the end-Cretaceous mass extinction in North America: Proceedings of the National Academy of Sciences of the United States of America, v. 109, p. 18857–18861, https://doi.org/10.1073/pnas.1202196109.

Montagnac, G., Cardon, H., Daniel, I., and Reynard, B., 2016, Structural changes in perylene from UV Raman spectroscopy up to 1 Gpa: Journal of Raman Spectroscopy: Journal of Raman Spectroscopy, v. 47, p. 720–725, https://doi.org/10.1002/jrs.4890.

Montagnac, G., Hao, J., Pedreira-Segade, U., and Daniel, I., 2021, Detection of nucleotides adsorbed onto clay by UV resonant Raman spectroscopy: A step towards the search for biosignatures on Mars: Applied Clay Science, v. 200, https://doi.org/10.1016/j.clay.2020.105824.

Moynier, F., and Fujii, T., 2017, Calcium isotope fractionation between aqueous compounds relevant to low-temperature geochemistry, biology and medicine: Scientific Reports, v. 7, 44255, https://doi.org/10.1038/srep44255.

Murphy, E.C., Hoganson, J.W., and Johnson, K.R., 2002, Lithostratigraphy of the Hell Creek Formation in North Dakota: Geological Society of America Special Paper, v. 361, p. 9–34, https://doi.org/10.1130/0-8137-2361-2.9.

O'Haver, T., 2021, peakfit.m, MATLAB Central File Exchange, https://www.mathworks.com/matlabcentral/fileexchange/23611-peakfit-m (retrieved 30 April 2021).

Olcott Marshall, A., and Marshall, C.P., 2015, Vibrational spectroscopy of fossils: Palaeontology, v. 58, no. 2, p. 201–211, https://doi.org/10.1111/pala.12144.

Oreska, M.P.J., and Carrano, M.T., 2019, Paleocommunity mixing increases with marine transgression in Dinosaur Park Formation (Upper cretaceous) vertebrate microfossil assemblages: Paleobiology, v. 45, p. 136–153, https://doi.org/10.1017/pab.2018.36.

Ostrom, P.H., Macko, S.A., Engel, M.H., and Russell, D.A., 1993, Assessment of trophic structure of Cretaceous communities based on stable nitrogen isotope analyses: Geology, v. 21, p. 491–494, https://doi.org/10.1130/0091-7613(1993)021 < 0491:AOTSOC>2.3.CO;2.

Passey, B.H., and Cerling, T.E., 2002, Tooth enamel mineralization in ungulates: Implications for recovering a primary isotopic time-series: Geochimica et Cosmochimica Acta, v. 66, p. 3225–3234, https://doi.org/10.1016/S0016-7037(02)00933-X.

Penel, G., Leroy, G., Rey, C., and Bres, E., 1998, MicroRaman spectral study of the PO 4 and CO 3 vibrational modes in synthetic and biological apatites: Calcified Tissue International, v. 63, no. 6, p. 475–481, https://doi.org/10.1007/s002239900561.

Pucéat, E., Reynard, B., and Lécuyer, C., 2004, Can crystallinity be used to determine the degree of chemical alteration of biogenic apatites?: Chemical Geology, v. 205, no. 1–2, p. 83–97, https://doi.org/10.1016/j.chemgeo.2003.12.014.

Reynard, B., and Balter, V., 2014, Trace elements and their isotopes in bones and teeth: Diet, environments, diagenesis, and dating of archeological and paleontological samples: Palaeogeography, Palaeoclimatology, Palaeoecology, v. 416, p. 4–16, https://doi.org/10.1016/j.palaeo.2014.07.038.

Rybczynski, N., and Vickaryous, M.K., 2001, Evidence of complex jaw movement in the Late Cretaceous ankylosaurid *Euoplocephalus tutus* (Dinosauria: Thyreophora), *in* Carpenter, K., ed., The Armored Dinosaurs: Bloomington, Indiana University Press, p. 299–317.

Sakamoto, M., Benton, M.J., and Venditti, C., 2016, Dinosaurs in decline tens of millions of years before their final extinction: Proceedings of the National Academy of Sciences of the United States of America, v. 113, p. 5036–5040, https://doi.org/10.1073/pnas.1521478113.

Schmitt, A.-D., 2016, Earth-surface Ca isotopic fractionations, *in* Gussone, N., et al., eds., Calcium Stable Isotope Geochemistry: Berlin, Heidelberg, Germany, Springer, p. 145–172, https://doi.org/10.1007/978-3-540-68953-9_5.

Skulan, J., and DePaolo, D.J., 1999, Calcium isotope fractionation between soft and mineralized tissues as a monitor of calcium use in vertebrates: Proceedings of the National Academy of Sciences of the United States of America, v. 96, p. 13,709–13,713, https://doi.org/10.1073/pnas.96.24.13709.

Skulan, J., DePaolo, D.J., and Owens, T.L., 1997, Biological control of calcium isotopic abundances in the global calcium cycle: Geochimica et Cosmochimica Acta, v. 61, no. 12, p. 2505–2510, https://doi.org/10.1016/S0016-7037(97)00047-1.

Sillen, A., 1986, Biogenic and diagenetic Sr/Ca in Plio-Pleistocene fossils of the Omo Shungura Formation: Paleobiology, v. 12, p. 311–323, https://doi.org/10.1017/S0094837300013816.

Tacail, T., Albalat, E., Télouk, P., and Balter, V., 2014, A simplified protocol for measurement of Ca isotopes in biological samples: Journal of Analytical Atomic Spectrometry, v. 29, p. 529–535, https://doi.org/10.1039/c3ja50337b.

Tacail, T., Le Houedec, S., and Skulan, J.L., 2020, New frontiers in calcium stable isotope geochemistry: Perspectives in present and past vertebrate biology: Chemical Geology, v. 537, p. 11,9471, https://doi.org/10.1016/j.chemgeo.2020.119471.

Terrill, D.F., Henderson, C.M., and Anderson, J.S., 2020, New application of strontium isotopes reveals evidence of limited migratory behaviour in Late Cretaceous hadrosaurs: Biology Letters, v. 16, https://doi.org/10.1098/rsbl.2019.0930.

Therrien, F., Zelenitsky, D.K., Voris, J.T., and Tanaka, K., 2021, Mandibular force profiles and tooth morphology in growth series of *Albertosaurus sarcophagus* and *Gorgosaurus libratus* (Tyrannosauridae: Albertosaurinae) provide evidence for an ontogenetic dietary shift in tyrannosaurids: Canadian Journal of Earth Sciences, v. 58, https://doi.org/10.1139/cjes-2020-0177.

Thomas, D.B., Fordyce, R.E., Frew, R.D., and Gordon, K.C., 2007, A rapid, non-destructive method of detecting diagenetic alteration in fossil bone using Raman spectroscopy: Journal of Raman Spectroscopy,v. 38, p. 1533–1537, https://doi.org/10.1002/jrs.1851.

Thomas, D.B., McGoverin, C.M., Fordyce, R.E., Frew, R.D., and Gordon, K.C., 2011, Raman spectroscopy of fossil bioapatite—a proxy for diagenetic alteration of the oxygen isotope composition: Palaeogeography, Palaeoclimatology, Palaeoecology, v. 310, p. 62–70, https://doi.org/10.1016/j.palaeo.2011.06.016.

Tipper, E.T., Schmitt, A., and Gussone, N., 2016, Global Ca cycles: Coupling of continental and oceanic processes, *in* Gussone, N., et al., eds., Calcium Stable Isotope Geochemistry: Berlin, Heidelberg, Germany, Springer, p. 173–222, https://doi.org/10.1007/978-3-540-68953-9_6.

Trayler, R.B., and Kohn, M.J., 2017, Tooth enamel maturation reequilibrates oxygen isotope compositions and supports simple sampling methods: Geochimica et Cosmochimica Acta, v. 198, p. 32–47, https://doi.org/10.1016/j.gca.2016.10.023.

Trueman, C., and Tuross, N., 2002, Trace elements in recent and fossilbone apatite, *in* Kohn, M.J., Rakovan, J., and Hughes, J.M., eds., Phosphates: Geochemical, Geobiological, and Materials Importance: Reviews in Mineralogy and Geochemistry, v. 48, p. 489–521.

Tütken, T., 2011, The diet of sauropod dinosaurs: implications of carbon isotope analysis on teeth, bones, and plants, *in* Klein, N., Remes, K., Gee, C.T., and Sander, P.M., eds., Biology of the Sauropod Dinosaurs, Understanding the Life of Giants: Bloomington and Indianapolis, Indiana, Indiana University Press, p. 57–79.

van der Merwe, N., and Medina, E., 1989, Photosynthesis and $^{13}C/^{12}C$ ratios in Amazonian rain forests: Geochimica et Cosmochimica Acta, v. 53, p. 1091–1094, https://doi.org/10.1016/0016-7037(89)90213-5.

Varricchio, D.J., 2001, Gut contents from a Cretaceous tyrannosaurid: Implications for theropod dinosaur digestive tracts: Journal of Paleontology, v. 75, p. 401–406, https://doi.org/10.1666/0022-3360(2001)075 < 0401:GCFACT>2.0.CO;2.

Vickaryous, M.K., Maryanska, T., and Weishampel, D.B., 2004, Ankylosauria, *in* Weishampel, D.B., Dodson, P., and Osmólska, H., eds., The Dinosauria (2nd edition): Berkeley, California, University of California Press, p. 363–392, https://doi.org/10.1525/california/9780520242098.003.0020.

Wang, Y., and Cerling, T.E., 1994, A model of fossil tooth and bone diagenesis: Implications for paleodiet reconstruction from stable isotopes: Palaeogeography, Palaeoclimatology, Palaeoecology, v. 107, p. 281–289, https://doi.org/10.1016/0031-0182(94)90100-7.

Weber, K., Weber, M., Menneken, M., Kral, A.G., Mertz-Kraus, R., Geisler, T., Vogl, J., and Tütken, T., 2021, Diagenetic stability of non-traditional stable isotope systems (Ca, Sr, Mg, Zn) in teeth—An in-vitro alteration experiment of biogenic apatite in isotopically enriched tracer solution: Chemical Geology, v. 572, 120196.

Weishampel, D.B., and Norman, D.B., 1989, Vertebrate herbivory in the Mesozoic; jaws, plants, and evolutionary metrics, *in* Farlow, J.O., ed., Paleobiology of the Dinosaurs: Geological Society of America Special Paper 238, p. 87–100, https://doi.org/10.1130/SPE238-p87.

Williamson, T.E., and Weil, A., 2008, Stratigraphic distribution of sauropods in the Upper Cretaceous of the San Juan Basin, New Mexico, with comments on North America's Cretaceous 'sauropod hiatus': Journal of Vertebrate Paleontology, v. 28, p. 1218–1223, https://doi.org/10.1671/0272-4634-28.4.1218.

Woodward, H.N., Tremaine, K., Williams, S.A., Zanno, L.E., Horner, J.R., and Myhrvold, N., 2020, Growing up *Tyrannosaurus rex*: Osteohistology refutes the pygmy "*Nanotyrannus*" and supports ontogenetic niche partitioning in juvenile *Tyrannosaurus*: Science Advances, v. 6, eaax6250, https://doi.org/10.1126/sciadv.aax6250.

Science Editor: Rob Strachan
Associate Editor: Brian Pratt

Manuscript Received 18 June 2021
Revised Manuscript Received 12 October 2021
Manuscript Accepted 10 November 2021

Printed in the USA